Studies on analysis of aryl hydrocarbon receptor (AhR) and HSP90 chaperone complex function

by
Ikuru Kudo

Department of Life Science
Graduate School of Engineering Science

Akita University

March 2018

Contents

List of publications

Papers Relevant and Related to the Present Study

1. Togashi S., Takahashi K., Tamura A., Toyota I., Hatakeyama S., Komatsuda A., Kudo I., Sasaki-Kudoh E., Okamoto T., Haga A., Miyamoto A., Grave E., Sugawara T., Shimizu H., Itoh H. (2017) High dose of antibiotic colistin induces oligomerization of molecular chaperine HSP90. *J. Biochemistry* **162**, 27-36.

2. Kudo I., Hosaka M., Haga A., Tsuji N., Nagata Y., Okada H., Fukuda K., Kakizaki Y., Okamoto T., Grave E., Itoh H. (2017) The regulation mechanisms of AhR by molecular chaperone complex. *J. Biochemistry* **mvx074**, 1-10.

3. Okamoto T., Yamamoto H., Kudo I., Matsumoto K., Odaka M., Grave E., Itoh H. (2017) HSP60 possesses a GTPase activity and mediates protein folding with HSP10. *Scientific Reports* **7**:16931.

Chapter I

General Introduction

1.1 Aryl hydrocarbon receptor

The aryl hydrocarbon receptor (AhR) is a member of the nuclear receptor superfamily and has the basic-loop-helix/Per-Arnt-Sim (bHLH/PAS) transcription factor [1-3]. AhR forms a complex with the molecular chaperone HSP90, co-chaperone p23, and the hepatitis B virus X-associated protein 2 (XAP2) in the cytoplasm [3,4]. AhR is the ligand-activated transcription regulator binding to environmental toxins with a high affinity such as 2,3,7,8-tetrachlorodibenzo-p-dioxin (TCDD) [3]. In the presence of ligand, AhR translocates into the nucleus and dimerizes with AhR nuclear translocater (ARNT), following a binding to the xenobiotic responsible element (XRE), the AhR/ARNT heterodimer induces the cytochrome P450 1A1 (CYP1A1), a toxicant metabolizing enzyme [5,6]. However, dioxin such as TCDD is accumulated *in vivo* without being metabolized because of the potent toxicity.

AhR consists of the N-terminal bHLH domain containing nuclear localization signal (NLS) and nuclear export signal (NES), the middle PAS-A and PAS-B domain includes a ligand binding site and the HSP90 binding site, and the C-terminal transactivation domain [7-9] (Fig.1). There are some reports about the association of AhR and HSP90 using *in vitro* transcription and translocation system in rabbit reticulocyte lysate or wheat germ lysate [10-12]. However, precise activation mechanisms of the AhR have not yet been fully understood *in vitro* due to the difficulty of the purification of AhR.

We have recently reported the direct interaction between the AhR-PAS domain and HSP90 using purified proteins [13]. HSP90 was dissociated from PAS in the presence of 17-DMAG, a inhibitor of HSP90. After ligand binding, HSP90 and AhR translocate from cytoplasm to nucleus while maintaining complex. Although the AhR-bHLH domain is known as a HSP90 binding domain [14], this direct protein-protein interaction has not yet been confirmed using purified proteins. In the present study, we investigated the direct interaction of AhR and HSP90 and/or co-chaperones using purified bHLH, HSP90, XAP2, and p23. We determined the bHLH binding domain of HSP90 using purified HSP90 domains. We also investigated the influence of HSP90 inhibitor on the interactions.

1.2 Molecular chaperone and HSP90

Molecular chaperones are the family of maintaining protein structure and function under various stress in living cells. Especially, heat shock proteins (HSPs), widely known as member of molecular chaperone, are induced to keep homeostasis when individuals, tissues, or cells are exposed to heat shock stress. Heat shock causes protein denaturalization or aggregation. If those proteins are not properly refolded or removed,

they sometimes accumulate and cause various protein-aggregation diseases like Alzheimer's disease, Parkinson's disease and age-associated disorders. HSPs were originally discovered when it was observed that chromosomal puffs were proposed by heat shock in the salivary glands of *Drosophilia* [15]. At present, it has been known that HSPs are also induced in several other risky situations, such as oxidative stress, exposure to chemical agents, physical agents (UV radiation), viral infections, anoxia, and ischemia [15,16].

HSP90 is one of the molecular chaperones, abundant and essential in eukaryotic cells. HSP90 regulates physiological functions of more than 300 proteins including AhR [13]. HSP90 consists of N-terminal ATP binding domain (N-domain), middle domain (M-domain), and C-terminal dimerization domain (C-domain) [17,18]. There are two major isoforms of HSP90α and HSP90β in mammalian cells. HSP90α is inducible under stress, while HSP90β is constitutively expressed. As a molecular chaperone, HSP90 use energy from ATP hydrolysis to fold newly synthesized proteins, aggregated proteins or misfolded proteins to the proper conformations in its homodimer cavity, cycling open-form and closed-form of conformational change.

1.3 AhR ligands

As mentioned above, dioxin TCDD is the most known ligand of AhR. There are also well studied ligands of AhR, grouped into polycyclic aromatic hydrocarbons (PAHs), polychlorinated biphenyls (PCBs), and halogenated dioxins and related compounds, reviewed by Stejskalova L. et al. [19]. Fig. 2 exhibits some of chemical structures of AhR ligands. Most of known AhR ligands are cellular toxic or potentially carcinogenic, due to not be metabolized by CYP family proteins or their metabolic production causes DNA damage. Recently, however, some studies focused on not only toxicity by AhR ligands but also its possibility for the immunostimulating effect [20,21]. Thus, we have focused on 1,4-dihydroxy-2-naphthoic acid (DHNA), a novel non-toxic ligand of AhR derived from *Propionibacterium freudenreichii* ET-3 isolated from Swiss-type cheese [22,23]. DHNA is proposed to be not or little toxic for human and mice according to the research of Generally recognized as safe (GRAS) in the U.S. Food & Drug administration (FDA) and Meiji dairies corporation, Japan. In this study, we examined molecular mechanism of AhR activation by DHNA in human cells.

Chapter II

Materials and Methods

Materials

17-(Dimethylaminoethylamino)-17-demethoxygeldanamysin (17-DMAG) as the inhibitor of HSP90 was purchased from Invitrogen (San Diego, U.S.A.). Isopropyl-1-thio-β-D-galactopyranoside (IPTG) was purchased from Nakarai Tesque (Kyoto, Japan). 3-methylcolanthrene (3MC) and 1,4-dihydroxy-2-naphthoic acid (DHNA) was purchased from Sigma-Aldrich Japan. Anti-HSP90β antibody (SPA-843) was purchased from Assay Designs (New York, U.S.A.), anti-AhR antibody (sc-5579) was purchased from Santa Cruz Biotechnology (Texas, U.S.A.), anti-β-actin antibody (A5441) was purchased from Sigma-Aldrich Japan, anti-IL12B p40 antibody (701233), Alexa Fluor 488 conjugated anti-mouse antibody and Alexa Fluor 546 conjugated anti-rabbit antibody were purchased from Invitrogen, anti-Interferon gamma antibody (EPR1108, ab133566) was purchased from Abcam. Alkaline phosphatase (AP) conjugated anti-mouse antibody (A3662), AP conjugated anti-rabbit antibody (A3687), and horse radish peroxidase (HRP) conjugated anti-mouse antibody (A9044) were purchased from Sigma-Aldrich Japan. HRP conjugated anti-rabbit antibody (#7074) were purchased from cell signaling technology.

Cell culture

Cervical tumor-derived HeLa cells were obtained from ATCC. Human colon carcinoma Caco-2 cells were obtained from RIKEN cell bank. Cells were cultured in plastic dishes (Greiner, Germany) containing DMEM medium (Sigma-Aldrich Japan) supplemented with 5% fetal bovine serum (FBS) at 37°C under 5% CO_2 and 95% humidity.

Immunofluorescence

HeLa cells grown on a cover slip were treated with the vehicle or 3 μM 3MC or DHNA for 2 hours, fixed in ice-cold methanol at 4°C for 15 minutes, washed three times with PBS, and incubated with 1% BSA in PBS at room temperature for 1 hour. After washing with PBS, the primary antibody against HSP90β, AhR, p23, or XAP2 (diluted in 1% BSA/PBS) was mounted on a cover slip at 4°C for 18 hours. The cells were washed three times with PBS, and incubated with an Alexa488- or Alexa546-conjugated secondary antibody for 3 hours at room temperature. Finally, the cells were washed three times with PBS, incubated with DAPI (4',6-diamidino-2-phenylindole) for 30 minutes, and mounted onto a slide glass with ProLong Gold antifade reagent (Invitrogen). Immunofluorescence images were obtained by the confocal laser microscopy (LSM780, Zeiss).

***In situ* proximity ligation assay (PLA)**

HeLa cells grown on a cover slip were treated with the vehicle or 3 μM 3MC or DHNA for 2 hours, fixed in ice-cold methanol at 4°C for 15 minutes, washed three times with PBS, and incubated with 1% BSA in PBS at room temperature for 1 hour. After washing with PBS, the primary antibody against HSP90β, AhR, p23, or XAP2 (diluted in 1% BSA/PBS) in the combination of HSP90β-AhR, HSP90β-p23, and HSP90β-XAP2 was mounted on a cover slip at 4°C for 18 hours. Then PLA was performed according to the manufacture's instruction (Invitrogen).

Plasmid constructions

PCR cycle was previously described [13]. cDNA of bHLH was amplified by PCR using the forward primer 5'-GTCGACATGGCTGAAGGAATCAAGTCAA-3' and reverse primer 5'-GCGGCCGCTCAATCAAAGAAGCTCTTGGCTCT-3'. The resulting PCR products were inserted into the Sal I/Not I sites of the pGEX-5X-3 vector. The constructs were confirmed by DNA sequencing. The cDNA of p23 was amplified by PCR using the forward primer 5'-CATATGCAGCCTGCTTCTGCAAAGTG-3' and reverse primer 5'-GAATTCTTACTCCAGATCTGGCATTTTT-3'. The resulting PCR products were inserted into the Nde I/EcoR I sites of the pET21a vector. The constructs were confirmed by DNA sequencing. cDNA of XAP2 was amplified by PCR using the forward primer 5'-CATATGGCGGATATCATCGCAAG-3' and reverse primer 5'-GAATTCTCAATGGGAGAAGATCCCC-3'. The resulting PCR products were inserted into the Nde I/EcoR I sites of the pET21a vector. The constructs were confirmed by DNA sequencing.

HSP90, HSP90 N-, M-, C-, ΔN-, ΔM-, and ΔC-domains were amplified by PCR using the following primers: HSP90 and HSP90 N-domain forward primer 5' -GGATCCATGCCTGAGGAAACCCAGACC-3', HSP90 and HSP90 C-domain reverse primer 5'- TCTAGATTAGTCTACTTCCATGCGTGA-3', HSP90 N-domain reverse primer 5'- TCTAGATTCAGCCTCATCATCGCGTGA-3', HSP90 C-domain forward primer 5'- GGATCCGGTTACATGGCAG-3', HSP90 M-domain forward primer 5'- CATATGCTCAACAAAACAAAGCCCATC-3', and HSP90 M-domain reverse primer 5'- CTCGAGTTCCAGGCCTTCTTTGGT-3'. The PCR products of HSP90, HSP90 N- and C-domains were digested with BamH I and Xba I restriction enzymes and cloned into the pCold I vector (TAKARA BIO, Inc. Japan). The PCR product of the HSP90 M-domain was digested with Nde I and Xho I restriction enzymes and cloned into the pET15b vector (Novagen, Inc. Japan).

Recombinant protein expression and purification

The bHLH was expressed in an *Escherichia coli* BL21 (DE3) arctic competent cell. The cells were grown at 37°C, 250 rpm in LB BROTH medium supplemented with 100 µg/ml ampicillin until the OD_{600} reached 0.5. The cells were then induced by the addition of 0.1 mM IPTG, and the culture medium was incubated at 37°C, 250 rpm for an additional 3 hr. The cells were harvested by centrifugation at 4°C, 13,000 rpm for 15 min, and cell pellets were suspended in 10 mM Tris-HCl pH 7.4. The cells were sonicated, centrifuged at 4°C, 15,000 rpm for 15 min and the formed pellets were collected. The collected pellets were suspended in buffer (1 M Arginine, 10 mM Tris-HCl pH 7.4), then dialyzed with 10 mM Tris-HCl pH7.4, overnight to remove the Arginine. After dialysis, the lysates were cleared by centrifugation at 4°C, 15,000 rpm for 15 min. The supernatant was applied to glutathione columns (Glutathione Sepharose 4B), washed with 10 mM Tris-HCl pH 7.4, and then eluted with elution buffer (20 mM Glutathione /10 mM Tris-HCl pH 7.4). Finally, the eluted proteins were concentrated by ultrafiltration.

The p23 was expressed in an *E. coli* BL21 (DE3) pLysS competent cell. The cells were grown at 37°C, 250 rpm in LB BROTH medium supplemented with 100 µg/ml ampicillin and 30 µg/l chloramphenicol until the OD_{600} reached 0.5. The cells were then induced by the addition of 0.5 mM IPTG, and the culture medium was incubated at 37°C, 250 rpm for an additional 3 hr. The cells were harvested by centrifugation at 4°C, 13,000 rpm for 15 min, and the cell pellets were suspended in 10 mM sodium acetate pH 6.0. The cells were sonicated, centrifuged at 4°C, 15,000 rpm for 15 min, then the supernatants were collected. Proteins were applied to the DEAE column, and then washed with 10 mM sodium acetate buffer pH 6.0/0.17 M NaCl. After washing, the proteins were eluted with a linear gradient of 0.17-0.6 M NaCl in 10 mM sodium acetate buffer pH 6.0. The p23 fractions were dialyzed overnight with 10 mM Tris-HCl pH 7.4. After dialysis, the lysates were applied to the Q-sepharose column. Then, washed with 10 mM Tris-HCl pH 7.4/0.1 M NaCl and the proteins were eluted with linear gradient of 0.1-0.6 M NaCl in 10 mM Tris-HCl pH 7.4. The collected protein fractions were concentrated by ammonium sulphate fractionation and 60-90% fractions were collected. The protein fractions were applied to the sephacryl column, and eluted with buffer (10 mM Tris-HCl pH 7.4/5% Glycerol/0.1 M NaCl). Finally, the collected fractions were concentrated by ultrafiltration.

The XAP2 was expressed in an *E. coli* BL21 (DE3) arctic competent cell. The cells were grown at 37°C, 250 rpm in LB BROTH medium supplemented with 100 µg/ml ampicillin until the OD_{600} reached 0.5. The culture medium was cooled for 30 min to

15°C. The cells were then induced by the addition of 0.5 mM IPTG and incubated at 15°C, 250 rpm for an additional 24 hr. The cells were harvested by centrifugation at 4°C, 13,000 rpm for 15 min, and cell pellets were suspended in 10 mM Tris-HCl pH 7.4. The cells were sonicated for two cycles, centrifuged at 4°C, 15,000 rpm for 15 min, then the supernatants were collected. Proteins were applied to the Heparin column, then washed with 10 mM Tris-HCl pH 7.4. After washing, the proteins were eluted with a linear gradient of 0-0.5 M NaCl in 10 mM Tris-HCl pH 7.4. The XAP2 fractions were dialyzed overnight with 10 mM Tris-HCl pH 7.4. After dialysis, collected proteins were applied to the Q-sepharose column, washed with 10 mM Tris-HCl pH 7.4. And then, proteins were eluted with a linear gradient of 0-0.6 M NaCl in 10 mM Tris-HCl pH 7.4. Finally, the eluted proteins were concentrated by ultrafiltration.

The HSP90 N-, M-, C-, ΔN-, ΔM-, and ΔC-domains were expressed as a 6×His fusion protein from the expression vector pCold I in the *E. coli* BL21 cells. The HSP90 M-domain was expressed as a 6×His fusion protein from the expression vector pET15b in the arctic express *E. coli* (DE3) cells. The expression of the HSP90 N-, M-, C-, ΔN-, ΔM-, and ΔC-domains were induced by 0.5 mM IPTG. The cells were collected and each of cell extracts was applied to the Ni-NTA column, washed and eluted as same as the other chaperones. The AhR-PAS domain was purified as previously described [13].

Antibody Production

An anti-p23 and anti-XAP2 antibody were produced by intramuscular injection into a rabbit of 1 mg of the purified each protein emulsified in complete Freund's adjuvant. Booster shots were given 3 times in the same manner as the original injection at 2-week intervals. The rabbit was bled 10 days after the last injection. The protocols for animal experimentation described in this paper were previously approved by the Animal Research Committee, Akita University School of Medicine; the “Guidelines for Animal Experimentation” of the University were completely adhered to in all subsequent animal experiments.

XRE Affinity chromatography and gel-shift assay

The synthetic oligonucleotide which consist of four-tandem repeats of human XRE or CY3-XRE [10 mer; (CY3) 5’-TTGCGTGCGG-3’] [24] were prepared (Fasmac Co., Ltd., Atsugi, Japan). XRE-Sepharose was prepared by coupling of XRE and Epoxy-activated Sepharose 6B (GE Healthcare Life Science) according to the manufacturer’s instructions. The purified GST-bHLH or GST were added to XRE-Sepharose or Mock (without XRE)-Sepharose column equilibrated with buffer (25

mM HEPES-KOH pH 7.4/5% Glycerol/0.1% NP-40/5 mM $MgCl_2$) and incubated with gentle rotation using a rotator for 30 min at 4°C. After washing with the same buffer three times, the bound proteins were separated by SDS-PAGE. Purified GST-bHLH (0.5 µM) and CY3-XRE (0.5 µM) were incubated with Binding Buffer (15 mM Tris-HCl pH 7.4, 75 mM NaCl, 1.5 mM EDTA, 1.5 mM DTT, 7.5% Glycerol, 0.5% NP-40) for 30 min at 4°C. Gel-shift assay was performed using 4% gel and gel-shift mobility was detected using ChemiDoc XRS+ (BioRad).

GST pull-down assay and 6×His pull-dowwn assay

For the GST pull-down assay, 2.5 µM GST-bHLH or GST protein was added to a solution of 2.5 µM HSP90, p23, XAP2, 1 mM ATP and 150 µl buffer A (0.1 M KCl/10 mM $MgCl_2$/20 mM Na_2MoO_4/0.6 M NaCl/5% Glycerol/0.1% NP-40 in 25 mM HEPES-KOH pH 7.4). The total volume of the sample was 300 µl by adding buffer B (5% Glycerol/0.1% NP-40 in 25 mM HEPES-KOH pH 7.4) and incubated using a rotator with gentle rotation at 37°C for 15 min. The samples were loaded onto a GST resin equilibrated with buffer C (50 mM KCl/5 mM $MgCl_2$/10 mM Na_2MoO_4/0.3 M NaCl/5% Glycerol/0.1% NP-40 in 25 mM HEPES-KOH pH 7.4) and incubated for 15 min at 4°C with gentle rotation followed by centrifuged at 4°C, 5,000 rpm for 10 sec to remove the supernatant. The beads were washed three times with buffer C and eluted by boiling at 100°C for 5 min in SDS sample buffer. GST pull-down samples were separated by SDS-PAGE and immunoblotting. An antibody against HSP90 was used as previously reported [13].

Ni^{2+} pull-down assay

For the Ni^{2+} pull-down assay, 2.5 µM HSP90, XAP2, p23 and 1 mM ATP was added to 150 µl buffer D (25 mM HEPES-KOH pH 7.4/40 mM Imidazole/0.1% NP-40) and buffer E (25 mM HEPES-KOH pH 7.4/0.1% NP-40) upto 300 µl of total volume. The sample was incubated using a rotator with gentle rotation at 37°C for 15 min. The incubated solution was loaded onto Ni^{2+}-Sepharose resin equilibrated with buffer F (25 mM HEPES-KOH pH 7.4/20 mM Imidazole/0.1% NP-40). After incubation for 15 min at 4°C with gentle rotation, centrifuged at 4°C, 5,000 rpm for 10 sec to remove the supernatant. The beads were washed three times with buffer F and eluted by boiling at 100°C for 5 min in SDS sample buffer. Ni^{2+} pull-down samples were separated by SDS-PAGE.

RNA isolation and reverse transcription-polymerase chain reaction (RT-PCR)

The total RNA was isolated from the cells treated with DMSO, 3MC or DHNA for 0, 2, 4, and 8 h using the RNeasy Mini Kit (Qiagen, Valencia, CA). The amount and purity of the total RNA for each sample were estimated by spectrophotometric analysis at A260 and A280. The RNA quality was determined by agarose gel electrophoresis following ethidium bromide staining. Aliquots of the total RNA were diluted in diethylpyrocarbonated (DEPC)-treated water and stored at −80 °C. RNA (2 μg) was used to synthesize the first strand complementary DNA (cDNA) with Super Script III First-Strand (Invitrogen) under the following general conditions: denaturation at 94 °C for 30 s, annealing at 55 °C for 30 s, and extension at 68 °C for 30 s for up to 40 cycles using iCycler (BioRad). The cDNAs were PCR-amplified by iCycler (BioRad) with the primers of CYP1A1 (forward, 5′-ACCACCAAGAACTGCTTAGCC-3′; reverse, 5′-GAAGAGTGTCGGAAG-3′), IL-12B (forward, 5'-CCAAGAACTTGCAGCTGAAG-3'; reverse, 5'-TGGGTCTATTCCGTTGTGTC-3'), IFN-γ (forward, 5'-TCAGCTCTGCATCGTTTTGG-3'; reverse, 5'-GTTCCATTATCCGCTACATCTGAA-3'), β-actin (forward, 5′-GCTCGTCGTCGACAACGGCTC-3′; reverse, 5′-CAAACATGATCTGGGTCATCTTCTC-3′). The PCR products were separated in 1-2% agarose gels and stained with ethidium bromide. The band ratios were quantified using Image J software (Drop of Wisdom) and normalized by β-actin.

Western blotting

Cells were collected in the RIPA buffer (50 mM Tris-HCl, 150 mM NaCl, 0.1% SDS, 1% Nonidet P-40, 0.5% sodium deoxycholate, protease inhibitor cocktail). Cell extracts were prepared by disruption of cells by sonication for 10–15 s on ice, and were subjected to SDS-PAGE and western blot analysis; separated proteins were blotted onto PVDF membranes, blocked by 5% non-fat dry milk/TBS-T, and incubated with primary antibodies over night. Then, membranes were washed with TBS-T, incubated with secondary antibodies at room temperature for 1 hour, and were washed with TBS-T. The signals were detected with an ECL chemiluminescence detection kit (GE healthcare lifesciences) on a chemiluminescence image analyzer (ChemiDoc XRS+, Bio-Rad) according to the supplier’s instructions.

Dot blot assay

Cell medium supernatant was collected by centrifugation at 4°C, 5,000 rpm for 5 minutes, spotted on PVDF membranes using a dot blotter (Advantec, Japan). The membranes were washed with TBS-T, blocked by 5% non-fat dry milk/TBS-T, and

incubated with primary antibodies over night. Then, membranes were washed with TBS-T, incubated with secondary antibodies at room temperature for 1 hour, washed with TBS-T, and signals were detected by alkaline phosphatase activity. Images were quantified using Image J software and normalized by CBB stained dots without blocking and antibodies.

Chapter III

Results

3.1 Co-localization of AhR / HSP90 complex in the nucleus

We have reported that AhR translocated from cytoplasm to nucleus with HSP90 under treatment with β-NF [13]. In the current study, we confirmed of AhR nuclear translocation with chaperone complex in the presence of 3MC or DHNA. As shown in Fig. 3A-C, we confirmed that the AhR-chaperone complex located in the nucleus in the presence of 3MC. Surprisingly, however, p23 did not translocate to the nucleus when DHNA was treated.

3.2 Purification of GST-bHLH and DNA-binding ability

The AhR activation mechanism is poorly understood in vitro. In the previous study, we have reported that the AhR-PAS domain is a HSP90 binding domain, and both AhR and HSP90 translocate to nuclear from cytoplasm [13]. The AhR-bHLH domain has nuclear localization signal (NLS) and nuclear export signal (NES), so necessary for the transport to the nucleus. The AhR-bHLH domain is known to be as the HSP90 binding domain [10, 11]. However, direct interactions between AhR-bHLH and HSP90 in vitro have not yet reported. In the present study, we focused on the AhR-bHLH domain, and analyzed relations between AhR-bHLH and the molecular chaperone HSP90.
GST-bHLH was expressed in *E. coli* for using in GST pull-down assay. A purification of GST-bHLH was carried out by GST affinity column chromatography. As shown in Fig. 4A, the purified bHLH, having about 33-kDa molecular mass, was a single protein band on SDS-PAGE. If bHLH has correct structure, it may be able to bind to XRE (also called dioxin responsible element). We analyzed the DNA-binding ability of bHLH using a XRE-Sepharose affinity column. Because of the 3' end of XRE has OH- groups, we prepared the XRE affinity resin using an Epoxy-activated Sepharose 6B. Epoxy-activated Sepharose 6B is useful resin to fix the OH-, or NH_2- groups. No protein bands were shown in mock-columns (Fig. 4B, lanes 1 and 3). Although almost of GST was not able to bind to XRE-Sepharose affinity resins (Fig. 4B, lane 2), certain amount of bHLH could bind to the affinity resin (Fig. 4B, lane 4). We also investigated the XRE binding ability of bHLH using gel mobility-shift assay (Fig. 4C). We could detect signals at higher end of the gels only in the presence of bHLH. No gel mobility-shift has been detected in the presence of GST. These results suggested that the purified bHLH possesses a DNA-binding ability.

3.3 AhR-bHLH domain binds to HSP90, XAP2, and p23

We investigated an association between bHLH and HSP90 by GST pull-down assay. As shown in Fig. 5A, HSP90 protein bands were detected in only GST-bHLH lanes, not

in GST lanes. These results showed that the AhR-bHLH domain is also a HSP90 binding domain as same as the AhR-PAS domain. Its interaction was not changed in the presence or absence of ATP. We analyzed an effect of 17-DMAG on the interaction (Fig. 5B). The interaction between bHLH and HSP90 was not also affected by 17-DMAG in the presence or absence of ATP. We also analyzed the effects of co-chaperones p23 and XAP2 to the bHLH-HSP90 complex on SDS-PAGE. No proteins bound to GST (Fig. 6A). We could detect of HSP90 and bHLH on SDS-PAGE, but XAP2 and p23 were difficult to detect, so confirmed in immune-blot using antibodies against HSP90, p23 and XAP2. The p23 and XAP2 protein bands were shown in GST-bHLH lanes (Fig. 6B). Thus, these results support that AhR-bHLH interacts with HSP90, p23 and XAP2 in the cytoplasm. Furthermore, the complex was not affected by ATP. We investigated HSP90 co-chaperone complex using Ni^{2+} pull-down assay. As shown in Fig. 7, 6×His-HSP90 binds to the Ni^{2+}-Sepharose resin. We could detect HSP90, XAP2, and p23 protein bands on SDS-PAGE in the absence or presence of ATP. These results suggested that HSP90 makes a complex with XAP2 and p23 and AhR-bHLH binds to HSP90 complex via HSP90.

3.4 bHLH binding domains of HSP90

HSP90 is composed from 3 domains. ATP binding domain (N domain), substrate binding domain (M domain), and dimerization domain (C domain) [25]. We constructed and purified HSP90 domains and investigated the bHLH binding domain of HSP90 (Fig. 8). The domain structure of human AhR was also shown in Fig. 1. At first, we analyzed interactions between the AhR-ΔAD binding domain of HSP90 using HSP90 domains (N-, M-, and C-domain) as control. We could detect that AhR-ΔAD bound to the HSP90N domain (Fig. 9A). Neither HSP90M nor HSP90C domain bound to AhR-PAS. Then, we investigated the interactions between bHLH and each HSP90 domain (N, M and C) using GST-pull down assay (Fig. 9B). No proteins bound to GST. On the contrary, HSP90 N-domain was pull-downed with bHLH. We could not detect other domains (HSP90 M-, and HSP90 C-domain) on SDS-PAGE. ATP did not affect the interaction. We also confirmed the binding of the bHLH domain to HSP90 using HSP90 deletion mutants (HSP90-ΔC, ΔM, and ΔN). As shown in Fig. 9C, no HSP90 deletion mutants were interacted with GST. Both HSP90-ΔC and -ΔM interacted with bHLH, but not HSP90-ΔN. (The same data were shown in Figures 9B and C). These data suggested that AhR-bHLH bound to the HSP90 N-domain.

3.5 Difference in the component of AhR-chaperone complex in toxic or non-toxic

ligand.

To investigate whether components of AhR-chaperone complex are different in the sort of AhR ligand as shown in Fig. 3, we employed *in situ* proximity assay (PLA). PLA only react if two proteins interact proximity. So in this system, we could confirm which proteins of complex bound each other, and translocated into the nucleus in the presence of 3MC or DHNA. As result, HSP90β-AhR, HSP90β-p23, and HSP90β-XAP2 components translocated to the nucleus by the treatment of 3MC, while HSP90β-AhR, HSP90β-XAP2, but not HSP90β-p23 components translocated to the nucleus by the treatment of DHNA (Fig. 10A-C). Put together the data of immunofluorescence (Fig. 3) and PLA (Fig. 10), these results suggested that components of AhR-HSP90 chaperone complex were different from each ligand; known form of complex consists of AhR-HSP90-p23-XAP2 translocates to the nucleus by toxic ligands, novel form of complex consists of AhR-HSP90-XAP2 translocates to the nucleus by non-toxic ligands.

3.6 Induction of CYP1A1 in the presence of AhR ligands.

We examined the induction of CYP1A1 in HeLa cells treated with 3MC and DHNA. Cells were treated with 3MC and DHNA for 1, 2, 4, 6, and 8 hours for RNA isolation and RT-PCR (Fig. 11A, B), for 12, 24 and 48 hours for protein isolation and western blotting (Fig. 11C). Transcription of CYP1A1 by the treatment of 3MC was increased in the time-dependent manner, while it was transiently induced until 6 hours then started to decrease after 8 hours by the treatment of DHNA. As same as this result, CYP1A1 induction in protein level was continuous in the presence of 3MC (12-48 h) but was transient (12-24 h) in the presence of DHNA. These results indicated that DHNA was more quickly metabolized or less toxic compare to the known toxic ligands like TCDD, β-NF and 3MC.

3.7 Immunostimulating effect of AhR activation

We investigated whether AhR ligands could induce IL-12 and IFN-γ to stimulate immune system. IL-12 and IFN-g are cytokines which could improve immune system via activation of T cells, Natural killer cells, and macrophages. We performed RT-PCR and dot blot assay to examine the production of IL-12 and IFN-γ. After treatment of 3MC or DHNA, transcription of IL-12 and IFN-γ were upregulated (Fig. 12A-C), their protein release to the culture medium was also increased within 12 hours (Fig. 12D and E). These results suggested that the activation of AhR would be involved not only with induction of CYP1A1 but also with the cytokine signal transduction.

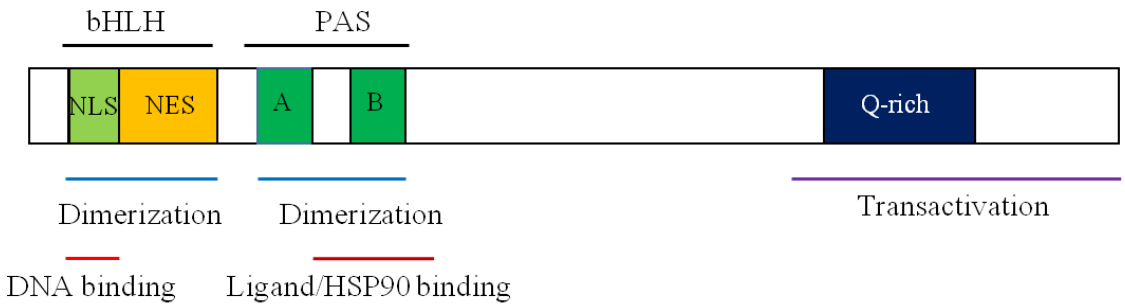

Figure 1. Domain structure of aryl hydrocarbon receptor (AhR).

AhR consists of the N-terminal bHLH domain containing nuclear localization signal (NLS) and nuclear export signal (NES), the middle PAS-A and PAS-B domain includes a ligand binding site and the HSP90 binding site, and the C-terminal transactivation domain.

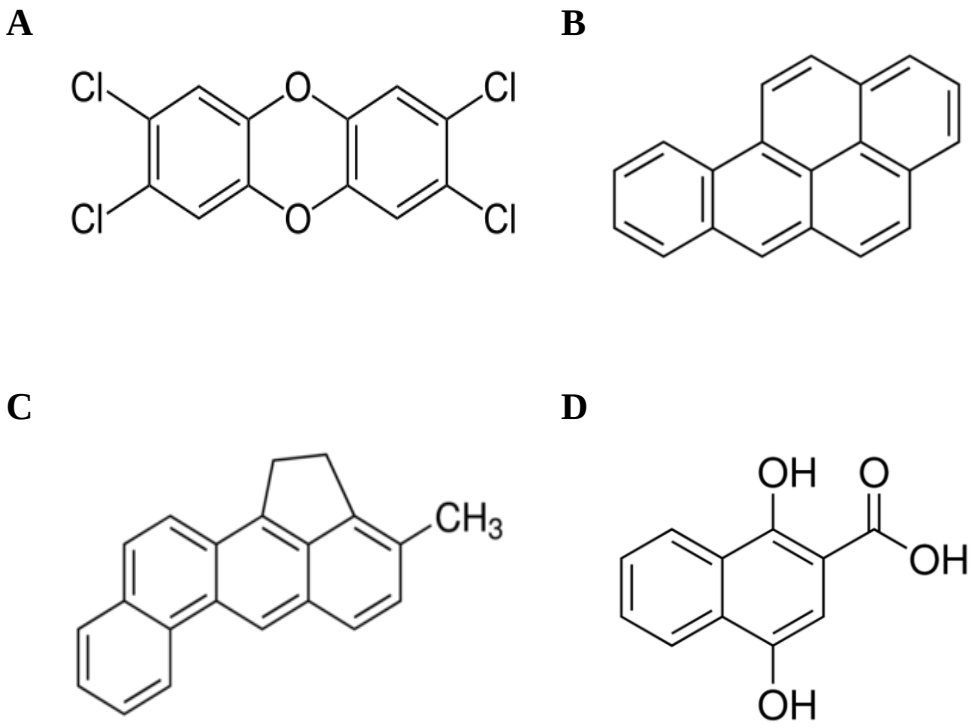

Figure 2. Chemical structures of AhR ligands.
(**A**) 2, 3, 7, 8-tetrachlorodibenzo-p-dioxin (TCDD), (**B**) Benzo(a)pyrene, (**C**) 3-methylcholanthrene (3MC), (**D**) 1,4-dihydroxy-2-naphotoic acid (DHNA).

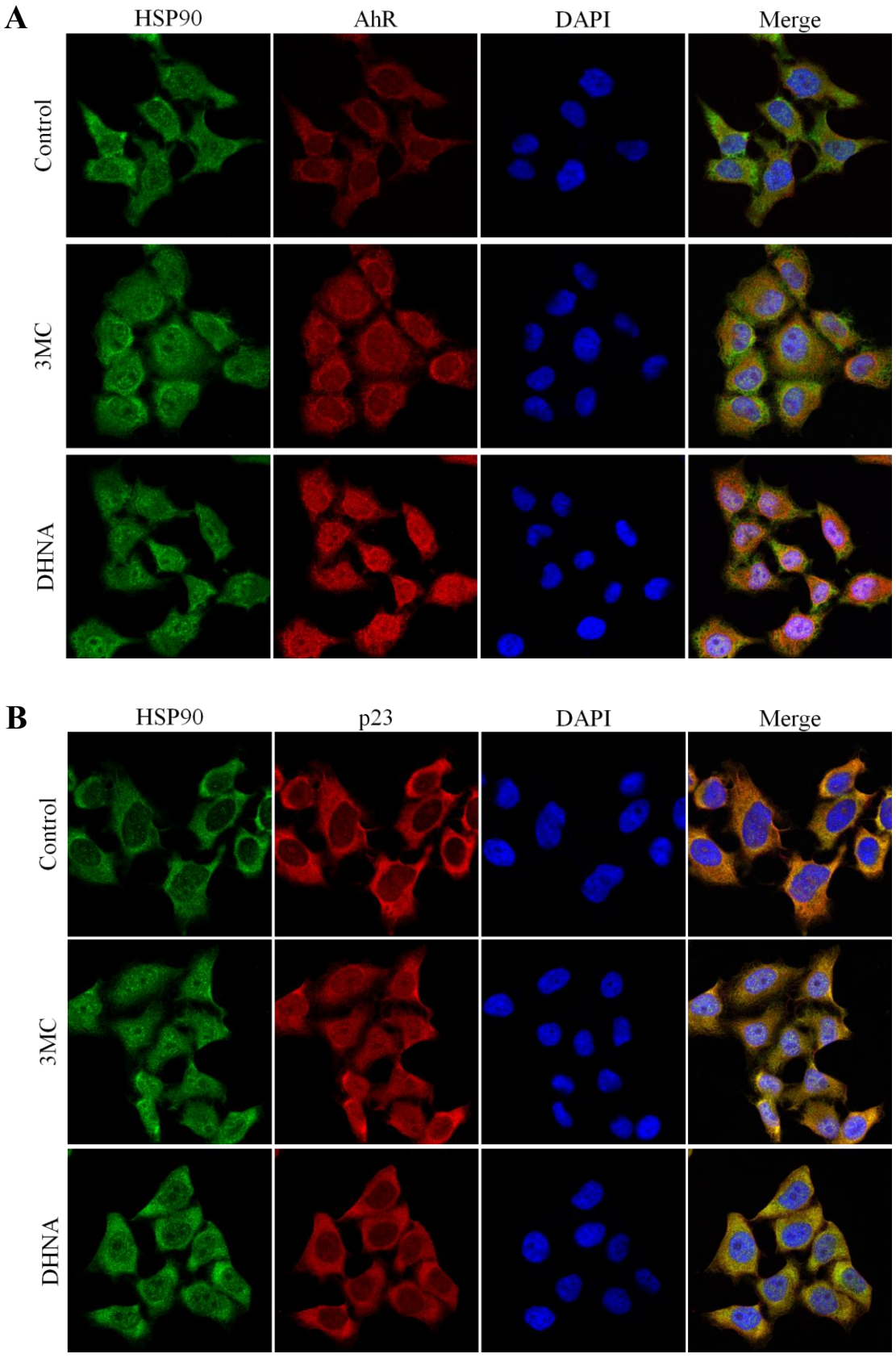
A
HSP90
AhR
DAPI
Merge
Control
3MC
DHNA
B
HSP90
p23
DAPI
Merge
Control
3MC
DHNA

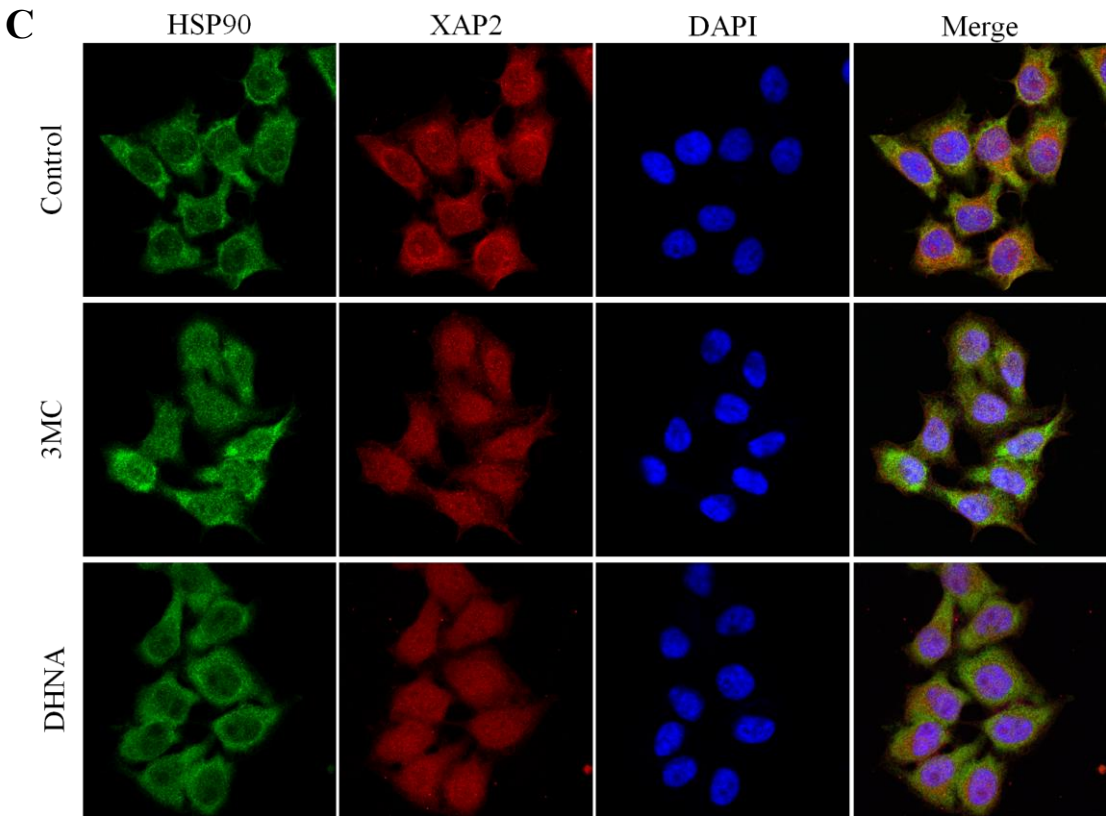

Figure 3. Co-localization of AhR and HSP90-chaperone complex.

HeLa cells were treated with the vehicle or 3 μM 3MC or 3 μM DHNA for 2 hours. Cells were incubated with anti-HSP90β and anti-AhR antibody (**A**), anti-HSP90β and anti-p23 antibody (**B**), and anti-HSP90β and anti-XAP2 antibody (**C**). Blue staining indicatees DAPI staining of cell nuclei (**A**-**C**). Images were taken at 630× magnification.

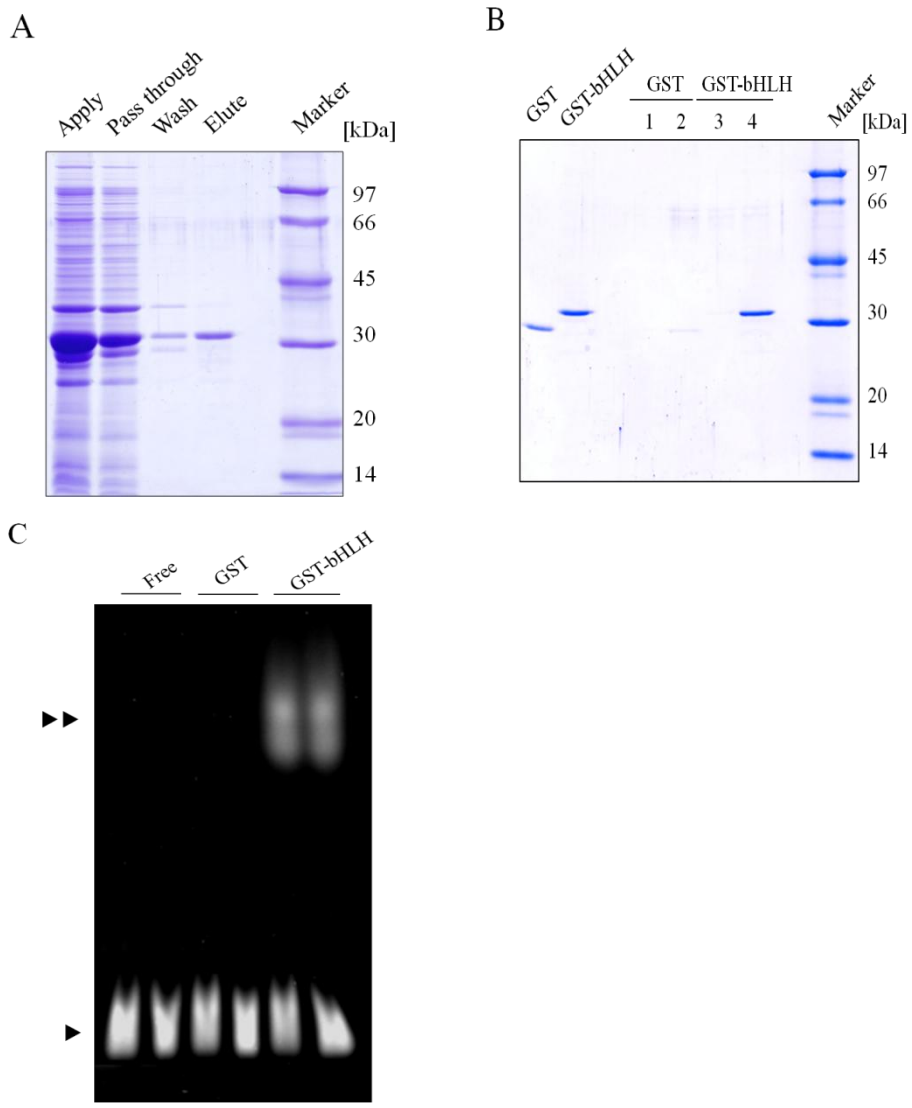

Figure 4. Purification of GST-bHLH.

(**A**) GST-bHLH was purified using a GST affinity column. Apply sample is supernatant after sonication of GST-bHLH expressed in *E. coli* and centrifugation. The column was washed with 10 mM Tris-HCl pH 7.4. GST and GST-bHLH were eluted by Glutathione. Eluted proteins were analyzed by SDS-PAGE (11% gel). (**B**) The purified protein and GST (input) were incubated with to Mock resin or XRE-Sepharose affinity resin at 4°C for 30 min, and the bound proteins were separated by SDS-PAGE (9% gel). Lanes 1, 3 and 2, 4 indicate Mock resins and XRE-Sepharose affinity resins, respectively. (**C**) The purified protein and GST (input) were incubated with CY3-XRE at 4°C for 30 min, samples were separated by SDS-PAGE (4% gel). Free, GST, and GST-bHLH indicates CY3-XRE, CY3-XRE/GST, and CY3-XRE/GST-bHLH, respectively. Single- and double-closed triangles indicate free and protein bound CY3-XRE, respectively.

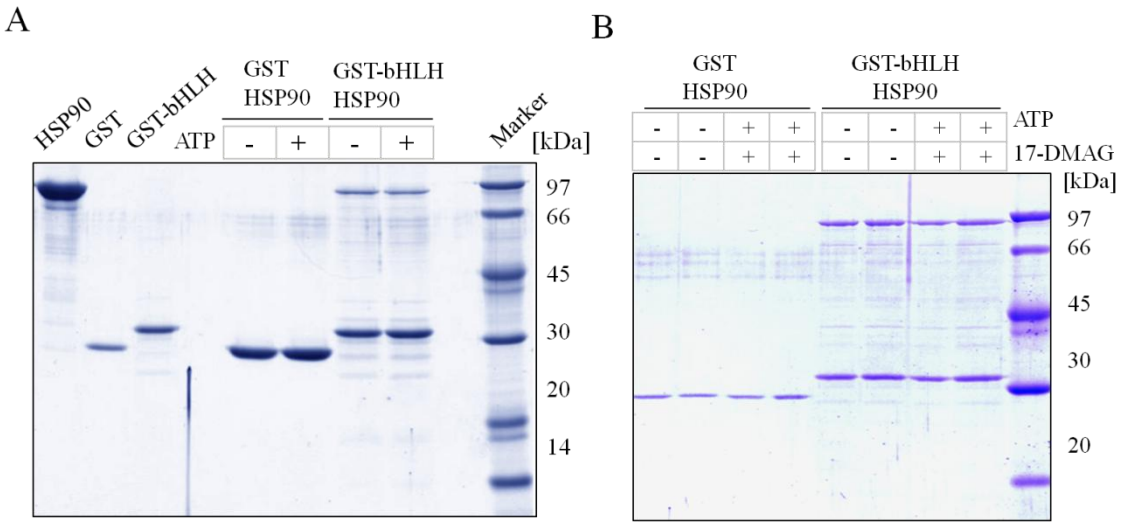

Figure 5. GST pull-down assay confirming the interaction of HSP90 with AhR-bHLH domain.

(**A**) An association between AhR-bHLH and HSP90 was analyzed by GST pull-down assay in the absence or presence of 1 mM ATP. GST-bHLH or GST, HSP90, and ATP were incubated with GST resins. After washing, Glutathione specific-binding proteins were analyzed by SDS-PAGE (11% gel). Lanes 1-3 of gels were the inputs from purified GST (28 kDa), GST-bHLH (33 kDa), and HSP90 (90 kDa) as a control, respectively. (**B**) The purified GST, GST-bHLH, and HSP90 were incubated with GST resins in the absence or presence of 50 μM 17-DMAG. The elutants from the glutathione columns were analyzed by SDS-PAGE (11% gel). Pull-down assays were performed using purified GST or the GST-AhR-PAS domain and purified HSP90 in the absence (-) or presence (+) of ATP.

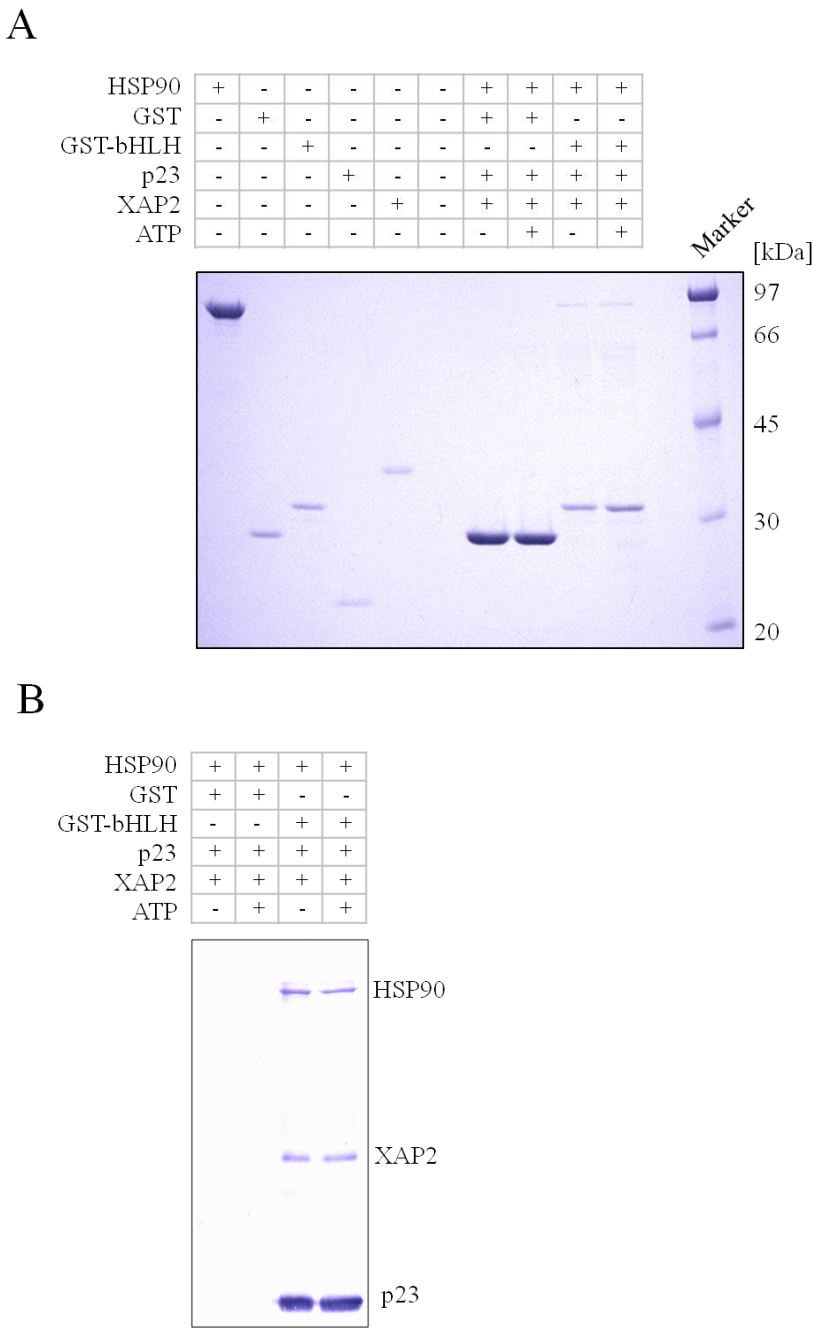

Figure 6. Conformational analysis of AhR, HSP90, and co-chaperone complex.

An AhR-bHLH binding protein was identified by GST pull-down assay. In the assay, GST resins were incubated with HSP90, p23, XAP2, and GST or GST-bHLH, in addition, in the absence or presence of 1 mM ATP. The binding proteins were analyzed by SDS-PAGE (9% gel) (**A**) or immunoblotting using anti-HSP90, anti-p23 and anti-XAP2 antibodies (**B**).

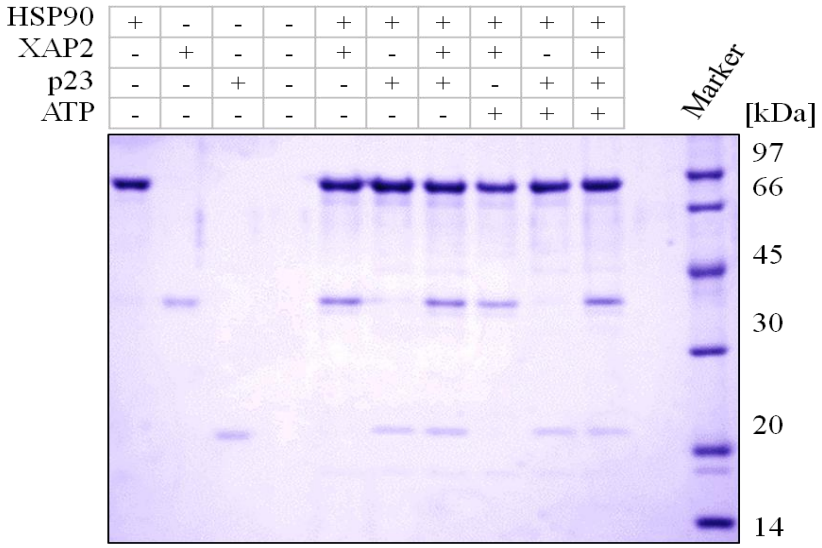

Figure 7. Conformational analysis of chaperone complex.

The HSP90 and co-chaperones binding properties were identified by Ni^{2+} pull-down assay. In the assay, Ni^{2+}-Sepharose resins were incubated with HSP90, p23, and XAP2 in the presence or absence of 1 mM ATP. The binding proteins were analyzed by SDS-PAGE (11% gel).

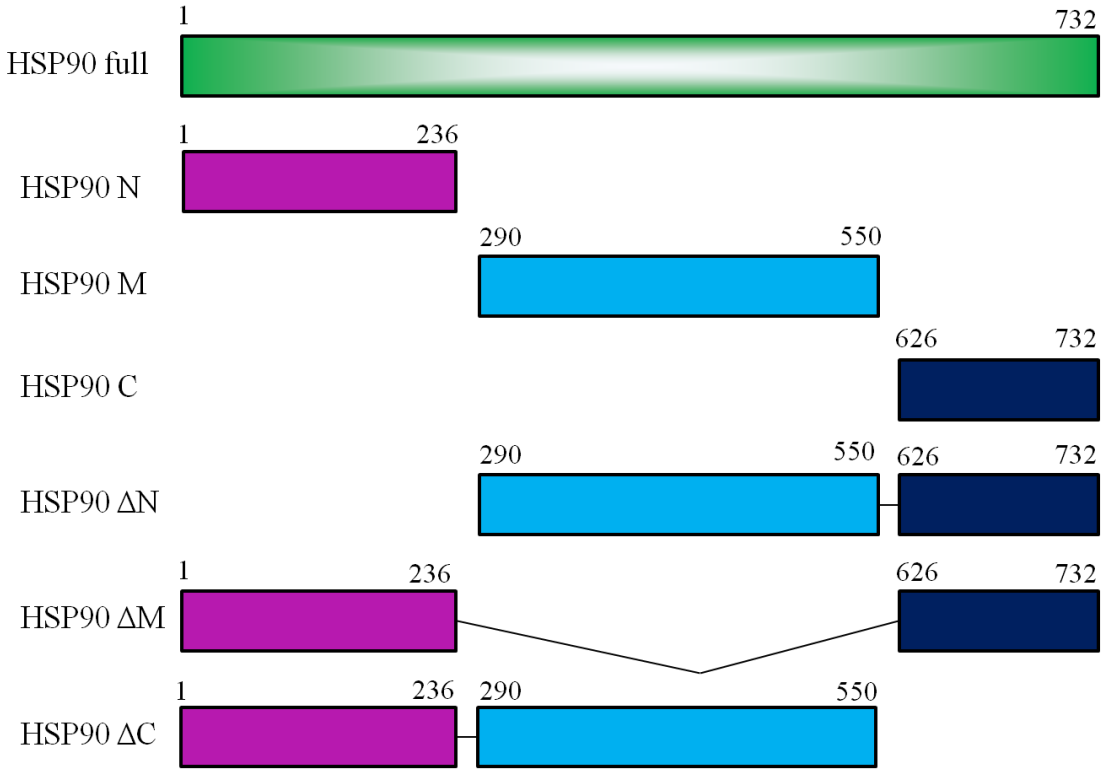

Figure 8. HSP90 domains.

Human HSP90 N-, M-, and C-domains or ΔN-, ΔM-, and ΔC-deletion mutants of HSP90 were constructed and purified under "Materials and Methods".

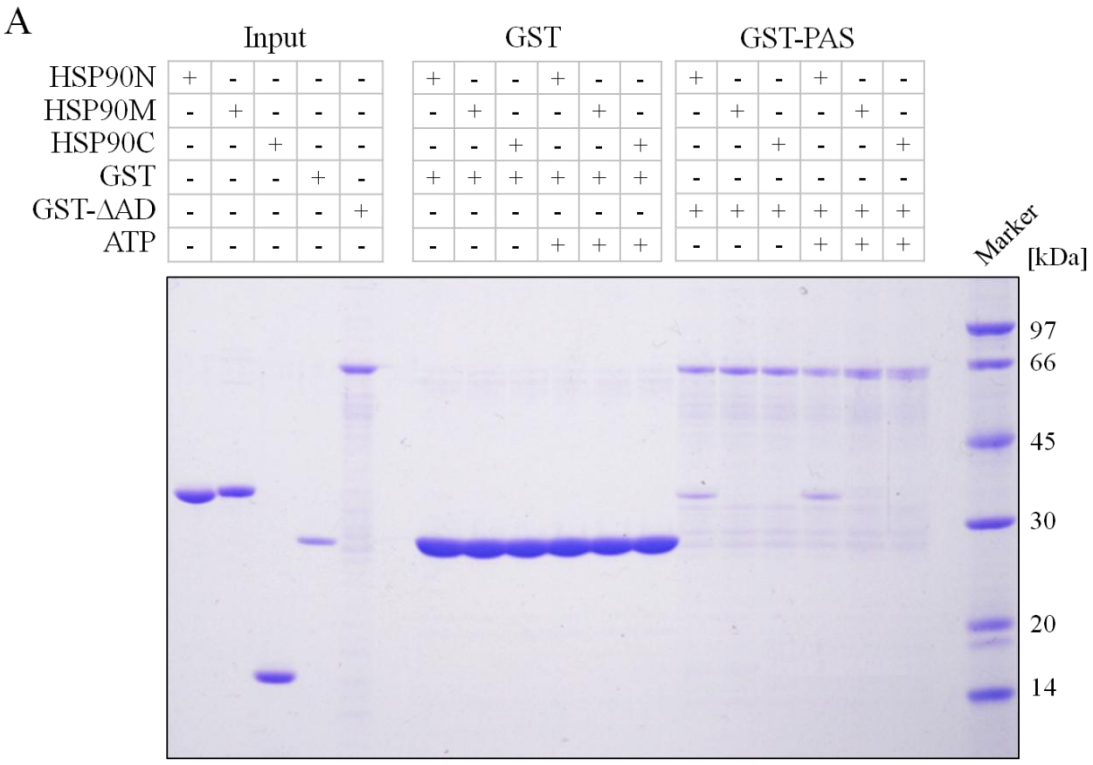
A
Input
GST
GST-PAS
HSP90N
HSP90M
HSP90C
GST
GST-ΔAD
ATP
Marker
[kDa]
97
66
45
30
20
14

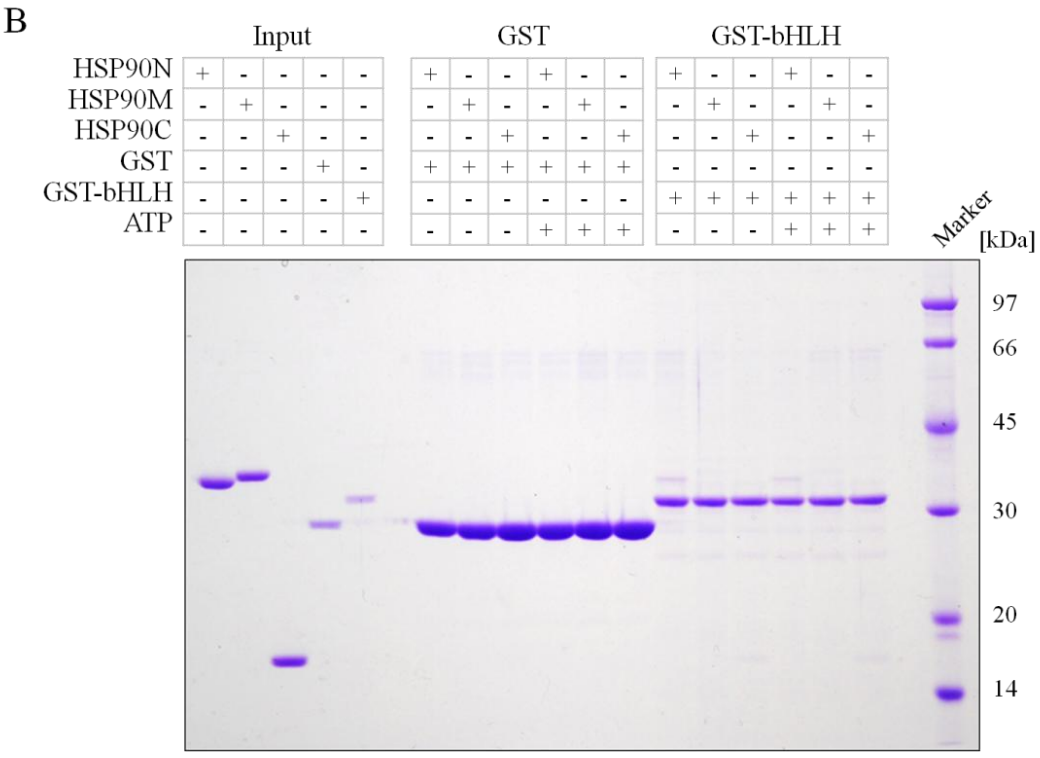
B
Input
GST
GST-bHLH
HSP90N
HSP90M
HSP90C
GST
GST-bHLH
ATP
Marker
[kDa]
97
66
45
30
20
14

C

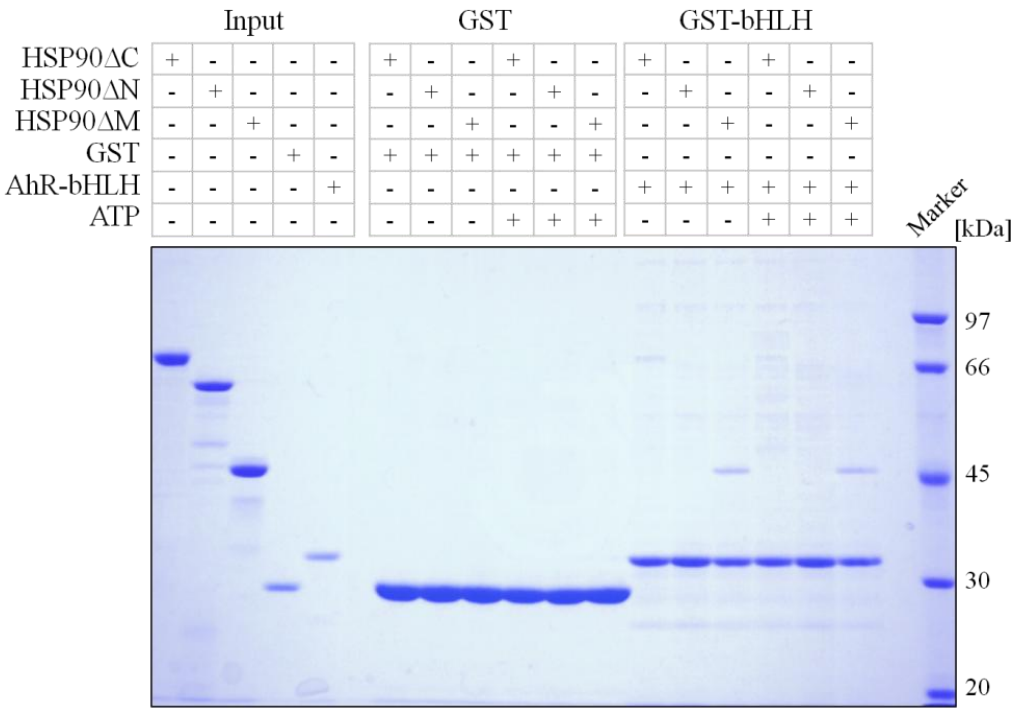
Input
GST
GST-bHLH
HSP90ΔC
HSP90ΔN
HSP90ΔM
GST
AhR-bHLH
ATP
Marker
[kDa]
97
66
45
30
20

D

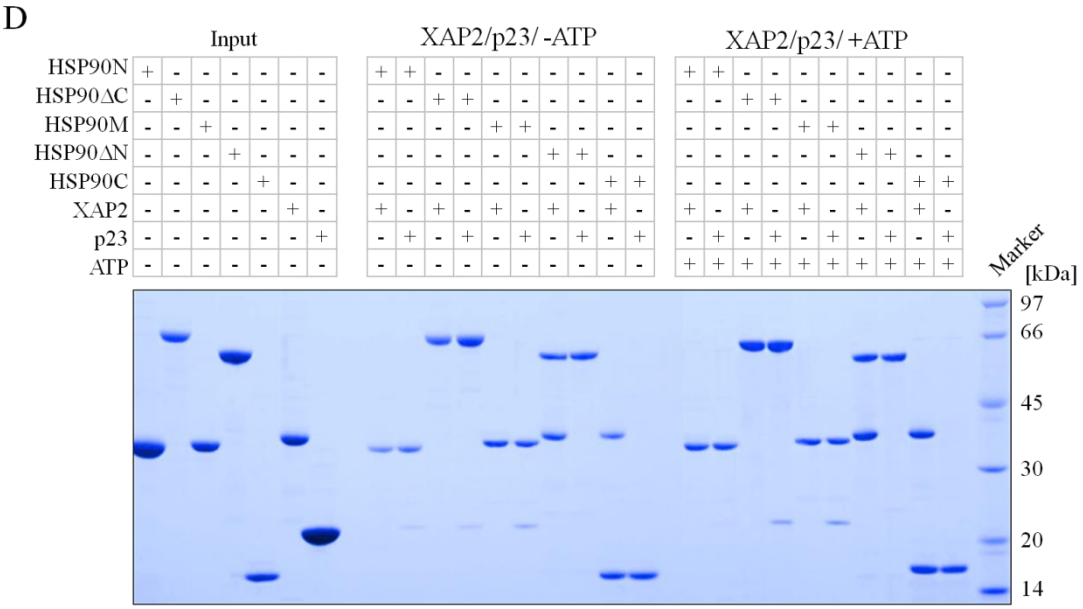
Input
XAP2/p23/-ATP
XAP2/p23/+ATP
HSP90N
HSP90ΔC
HSP90M
HSP90ΔN
HSP90C
XAP2
p23
ATP
Marker
[kDa]
97
66
45
30
20
14

Figure 9. GST pull-down assay confirming the interaction of HSP90N-, M-, and C-domains and GST-ΔAD or GST-bHLH.

(**A**) Purified GST, GST-ΔAD, HSP90 N-, M-, and C-domain were incubated with GST resins in the absence or presence of ATP. The elutants from the glutathione column were analyzed by SDS-PAGE (11% gel). Lanes 1-5 of gels were the inputs from purified HSP90 N-domain (38 kDa), HSP90 M-domain (40 kDa), HSP90 C-domain (16 kDa), GST (28 kDa), and GST-ΔAD (57 kDa) as a control, respectively. Pull-down assays were performed using purified GST (lanes 6-11) or the GST-AhR-ΔAD domain (lanes 12-17) and purified HSP90 in the absence (-) or presence (+) of ATP. (**B**) The purified GST, GST-bHLH, HSP90N-, M-, and C-domains were incubated with GST resins in the absence or presence of ATP. The elutants from the glutathione columns were analyzed by SDS-PAGE (11% gel). Lanes 1-5 of gels were the inputs from purified HSP90 N-domain (38 kDa), HSP90 M-domain (40 kDa), HSP90 C-domain (16 kDa), GST (28 kDa), and GST-bHLH (33 kDa) as a control, respectively. Pull-down assays were performed using purified GST or the GST-AhR-PAS domain and purified HSP90 in the absence (-) or presence (+) of ATP. (**C**) The purified GST, GST-bHLH, HSP90ΔN-, ΔM-, and ΔC-deletion mutants were incubated with GST resins in the absence or presence of ATP. The elutants from the glutathione columns were analyzed by SDS-PAGE (9% gel). Lanes 1-5 of gels were the inputs from purified HSP90ΔN (68 kDa), HSP90ΔC (60 kDa), HSP90ΔM (45 kDa), GST (28 kDa), and GST-bHLH (33 kDa) as a control, respectively. Pull-down assays were performed using purified GST or the GST-AhR-PAS domain and purified HSP90 in the absence (-) or presence (+) of ATP. **(D)** Ni^{2+} pull-down assays were performed as described in the "Materials and Methods". The purified HSP90N-, M-, C-domain, HSP90ΔN-, ΔC-deletion mutants, XAP2, and p23 were incubated with Ni^{2+}-Sepharose resin in the absence or presence of ATP. Ni^{2+} pull-down samples were analyzed by SDS-PAGE (11% gel). Lanes 1-7 of gels were the inputs from purified HSP90N-domain (38 kDa), HSP90ΔC (60 kDa), HSP90 M-domain (40 kDa), HSP90ΔN (68 kDa), HSP90 C-domain (16 kDa), XAP2 (38 kDa), and p23 (23 kDa) as a control, respectively. Ni-NTA pull-down assays were performed using purified HSP90N-domain, HSP90ΔC, HSP90M-domain, HSP90ΔN, and HSP90C-domain in the absence (-) or presence (+) of ATP.

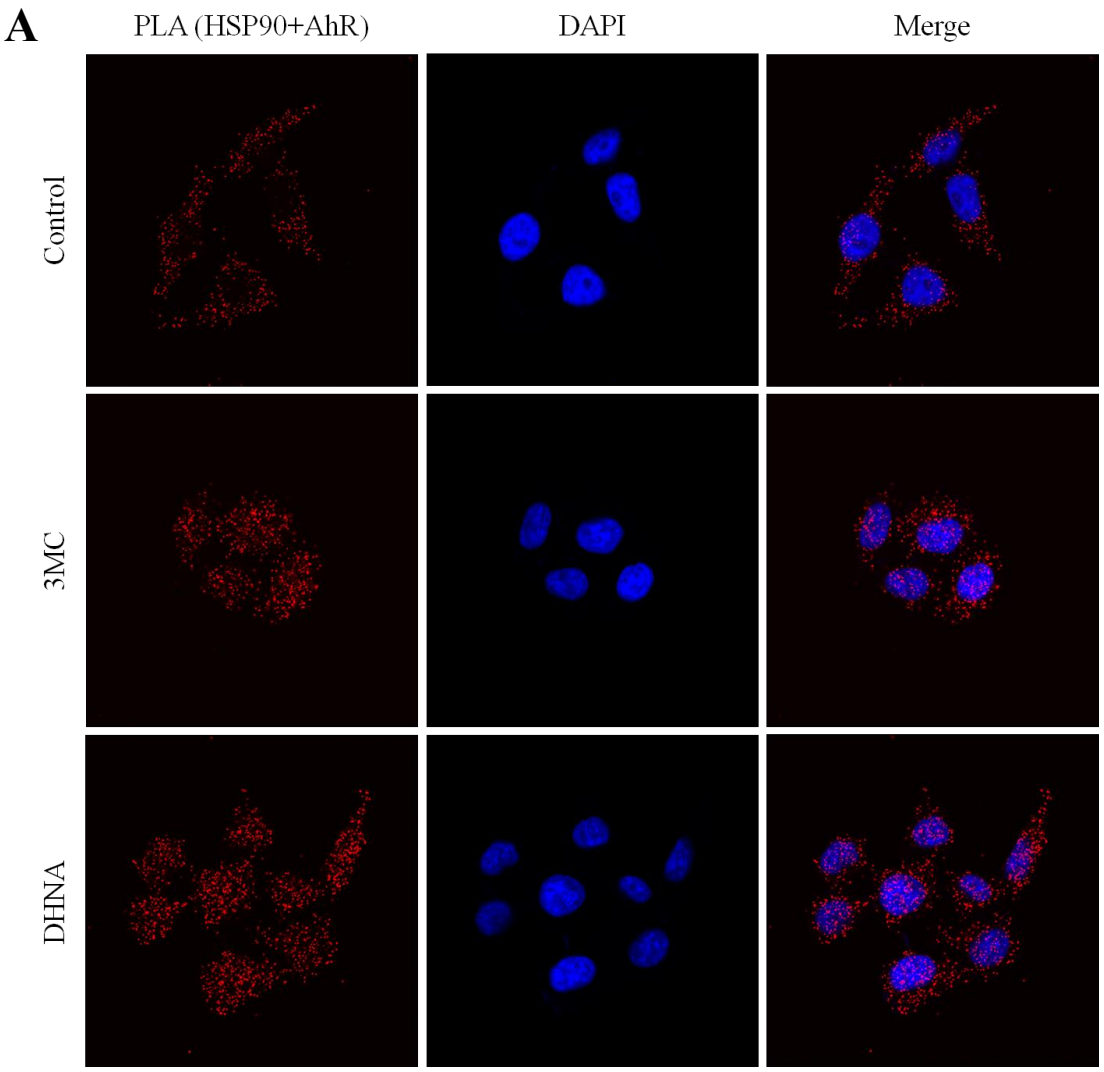
A
PLA (HSP90+AhR)
DAPI
Merge
Control
3MC
DHNA

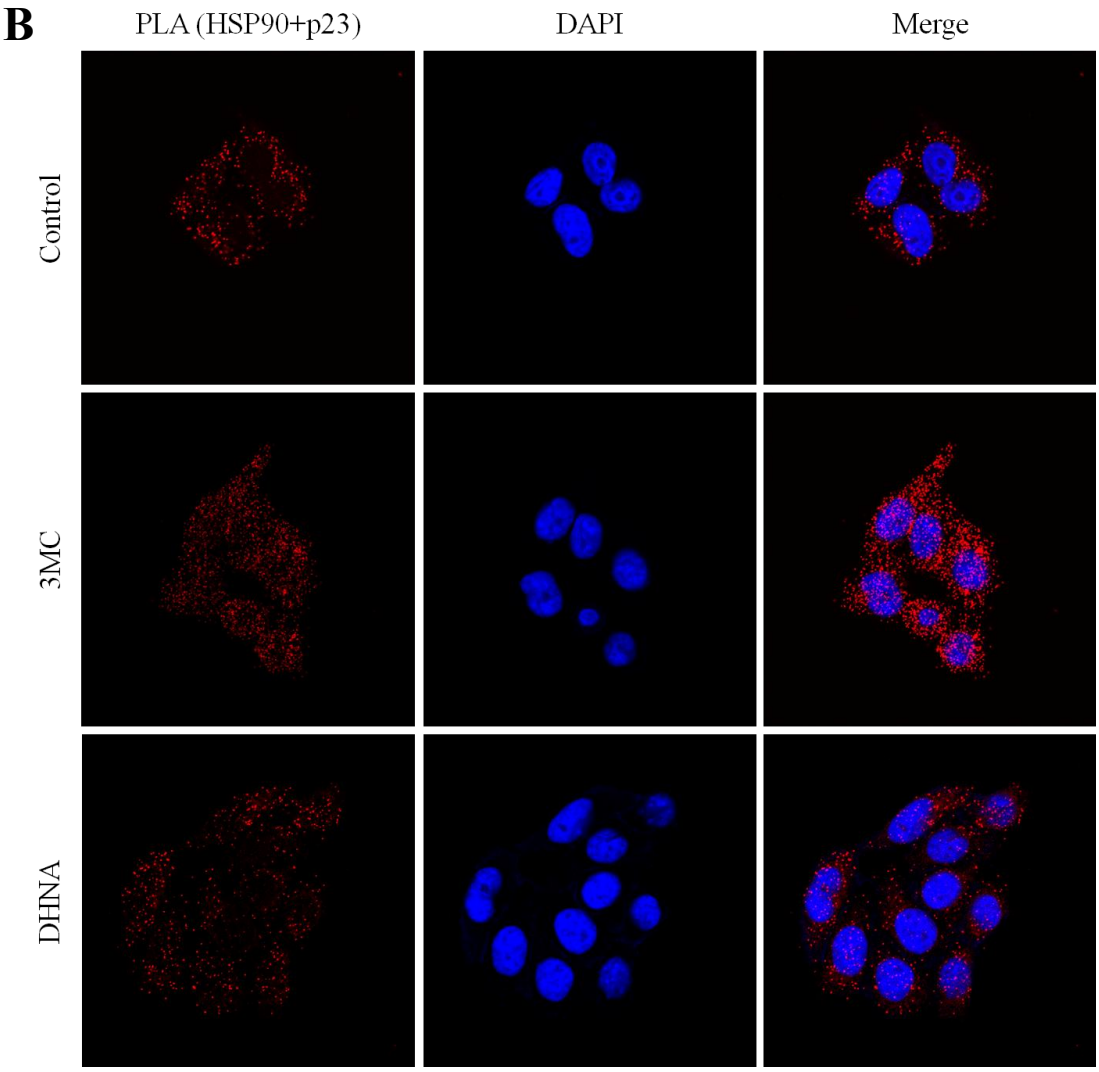
B
PLA (HSP90+p23)
DAPI
Merge
Control
3MC
DHNA

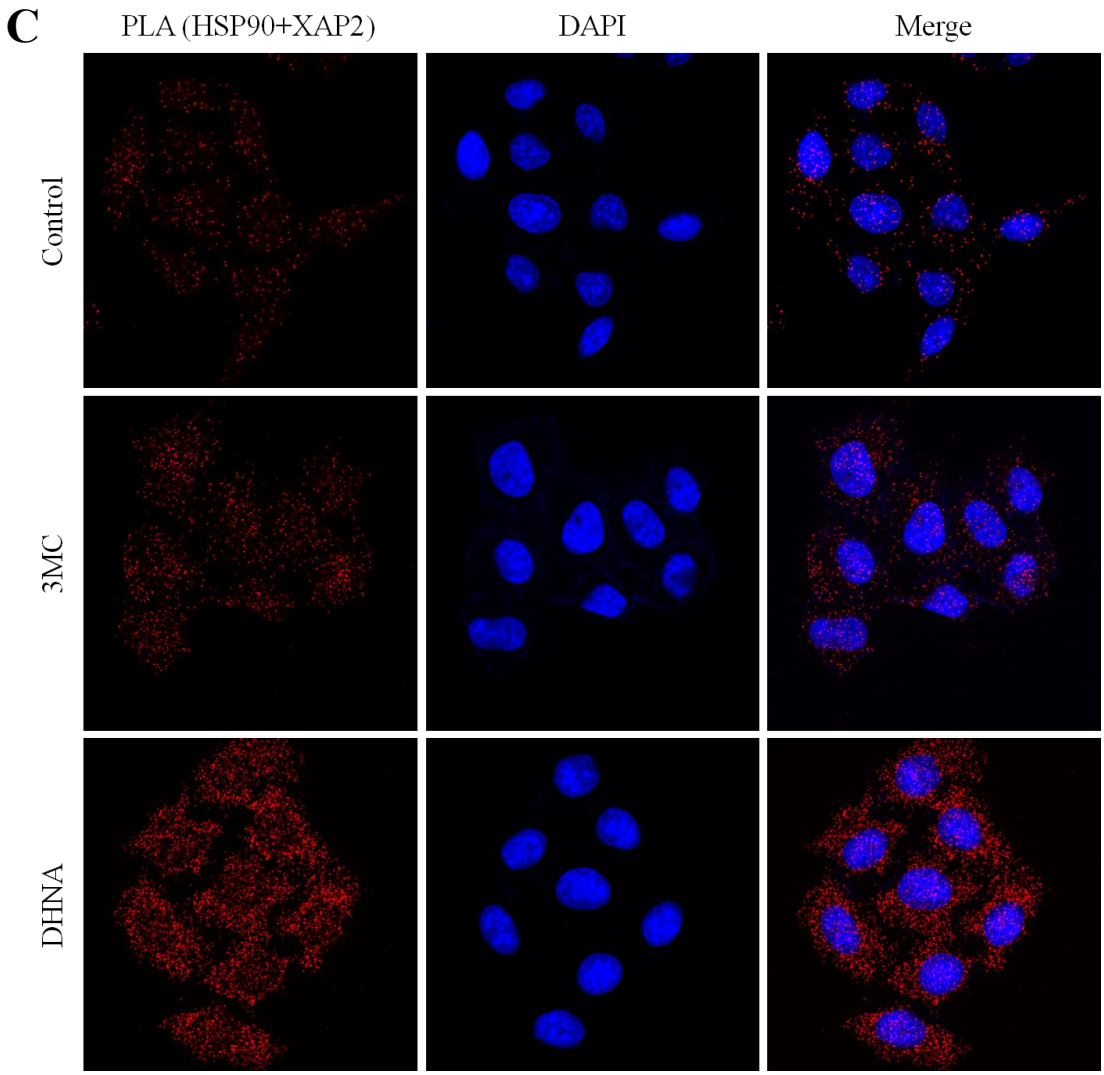

Figure 10. Ligand dependant co-localization of AhR and HSP90-chaperone complex.

HeLa cells were treated with the vehicle or 3 μM 3MC or 3 μM DHNA for 2 hours. Cells were incubated with anti-HSP90β and anti-AhR antibody (**A**), anti-HSP90β and anti-p23 antibody (**B**), and anti-HSP90β and anti-XAP2 antibody (**C**), followed by PLA. Red dots show the signal of PLA. Blue staining indicates DAPI staining of cell nuclei (**A**-**C**). Images were taken at 630× magnification.

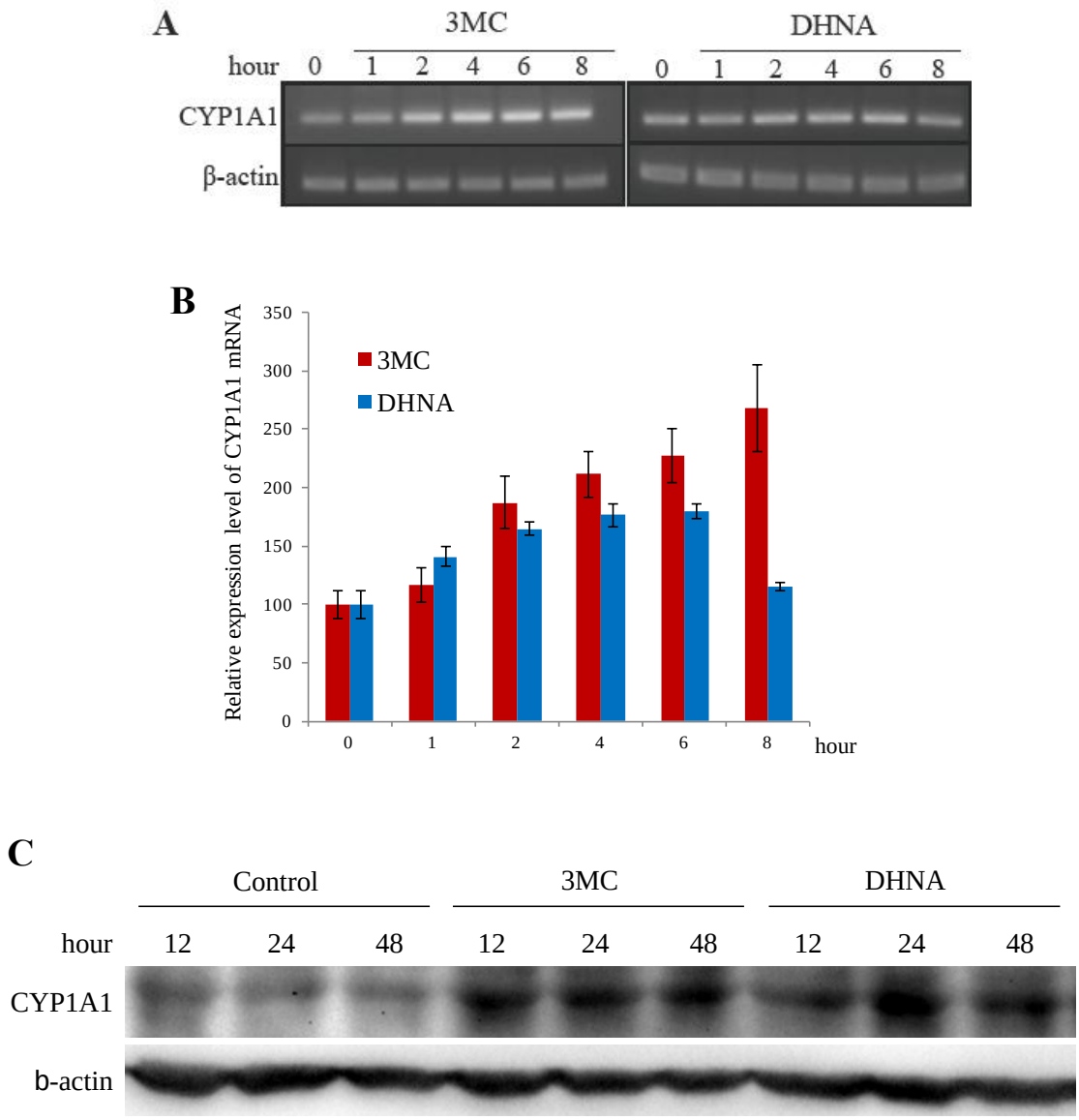

Figure 11. RT-PCR and western blot analysis of CYP1A1 expression in HeLa cells treated with 3MC or DHNA.

HeLa cells were treated with the vehicle or 3 μM 3MC or 3 μM DHNA for indicated hours and harvested for RT-PCR (**A, B**) and western blotting (**C**). Values represent the means ± s.d. (n=3).

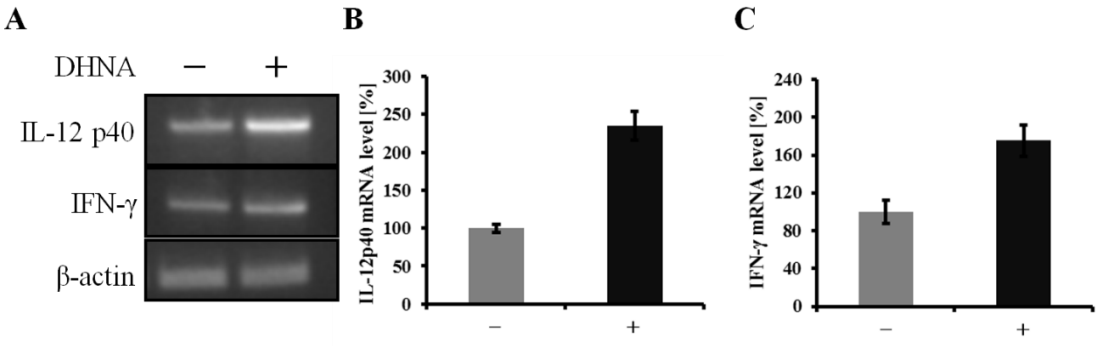
A
DHNA
−
+
IL-12 p40
IFN-γ
β-actin
B
IL-12p40 mRNA level [%]
300
250
200
150
100
50
0
−
+
C
IFN-γ mRNA level [%]
240
200
160
120
80
40
0
−
+

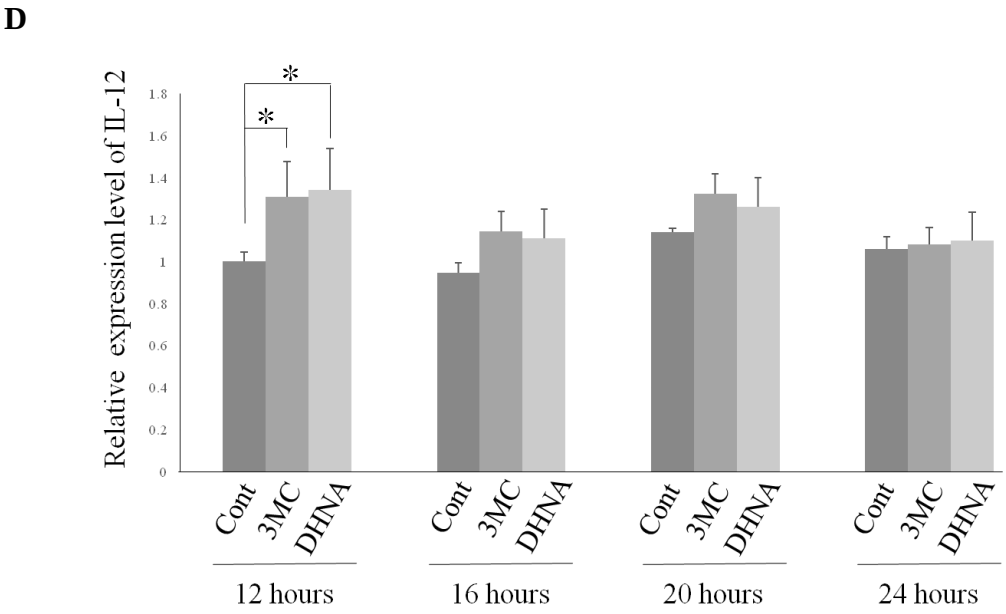
D
Relative expression level of IL-12
1.8
1.6
1.4
1.2
1
0.8
0.6
0.4
0.2
0
*
*
Cont
3MC
DHNA
12 hours
16 hours
20 hours
24 hours

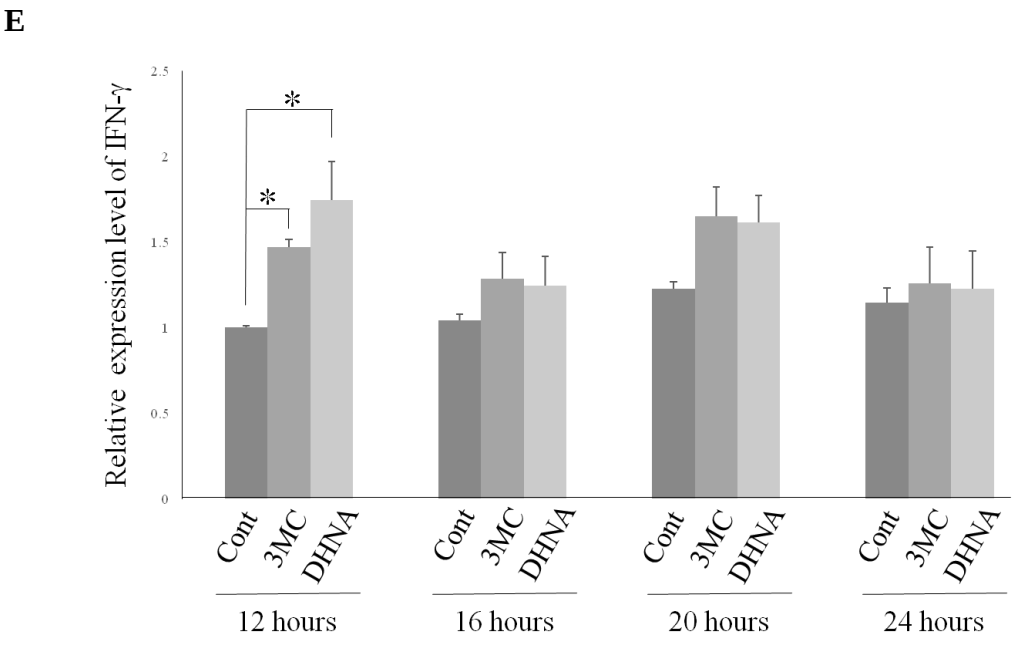
E
Relative expression level of IFN-γ
2.5
2
1.5
1
0.5
0
*
*
Cont
3MC
DHNA
12 hours
16 hours
20 hours
24 hours

Figure 12. Induction of IL-12 and IFN-γ by treatment of AhR ligands in Caco-2 cells.

Caco-2 cells were treated with 3MC or DHNA. After incubation of indicated times, cells were harvested and subjected to RT-PCR (**A-C**) and dot blot analysis (**D and E**). **A**, **B** and **D** shows expression levels of IL-12 p40. **A**, **C** and **E** shows expression levels of IFN-γ. Values represent the means ± s.d. (n=3, ✻: $p<0.05$).

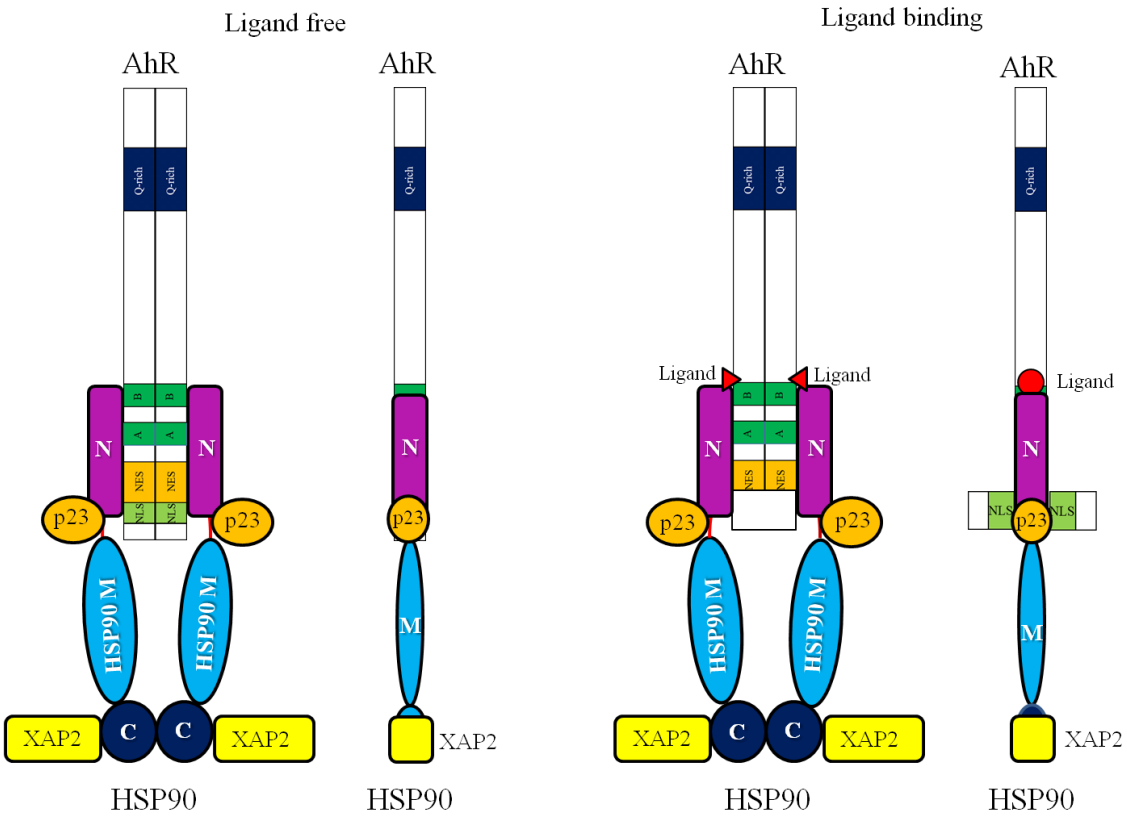

Figure 13. Conformational change models of the AhR, HSP90, p23, XAP2 complex.
The bHLH and PAS domains of AhR bind to HSP90 N-domain. Co-chaperones p23 and XAP2 bind to HSP90 N- and C-domains, respectively. When in the absence of ligand, the NLS of bHLH is hidden. When the ligands bind to AhR, the conformational changes will be occurred, then the NLS will be opened.

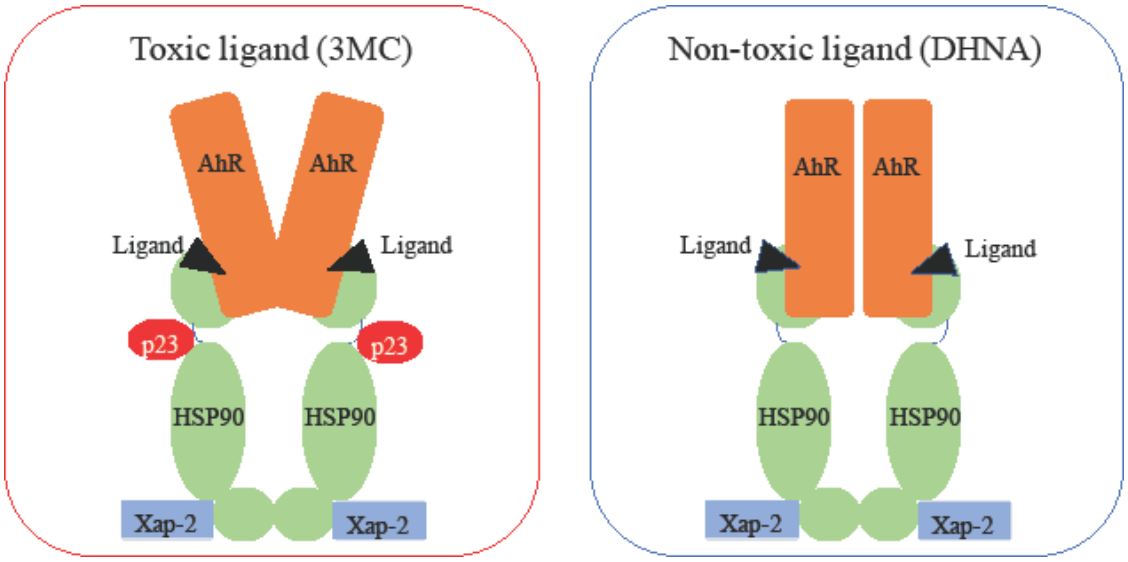

Figure 13. Model of difference in components of AhR, HSP90, p23, XAP2 complex.
In the presence of toxic ligands such as 3MC, the complex consists of AhR, HSP90, p23 and XAP2 (left model) for the nuclear translocation. In the presence of non-toxic ligands such as DHNA, the complex consists of AhR, HSP90 and XAP2 (right model) for the nuclear translocation. We think the presence or absence of p23 causes subtle conformation change of the complex for the ligand binding.

Chapter IV

Discussion

Discussion

4.1 *In vitro* analysis of AhR-bHLH and HSP90 complex binding.

The AhR activation mechanism has not yet been fully understood. AhR exists with HSP90, co-chaperone p23 and XAP2 in the cytoplasm. AhR has PAS and bHLH domains. The PAS domain is a ligand binding domain and a HSP90 binding domain. Recently, we have reported that the PAS domain binds to HSP90 directly [13]. Because of the difficulty to purify the full length of AhR, we used some purified domains of AhR for experiments. We purified the PAS domain and checked the ligand-binding ability of purified the PAS domain using a β-naphthoflavone (β-NF) affinity resin. In this study, we investigated whether AhR-bHLH bound to HSP90, p23 and XAP2 or not. The AhR-bHLH domain has NLS, NES and the XRE binding domain. Moreover, the AhR-bHLH domain has been thought to be a HSP90 binding domain. First, we confirmed that purified AhR-bHLH protein bound to XRE. In the present study, we used XRE affinity resins. An oligonucleotide has OH- group in the 3' end. We fixed the four tandem XRE to Epoxy Sepharose 6B columns. The affinity resin is able to fix the OH- or NH_2- group of protein, ligand, and DNA. Until now, we have a number of reports in the drug-affinity [26-29]. The purified bHLH could bind to XRE affinity resins, but not mock resins. GST did not bind to either XRE affinity resins or mock resins. We also analyzed the interaction between DNA and protein using gel mobility-shift assay. We used CY3-XRE at the methods. GST didn't show the interaction. On the contrary, we could detect the gel mobility-shift between CY3-XRE and GST-bHLH. Thus, we confirmed the purification of functional bHLH.

So far some of the detail of the interaction between AhR and HSP90 has been published. However, few data showed direct relations in molecular level. A nucleotide binding to the HSP90 N-domain induces a directionality and a conformational cycle. In the absence of ATP, HSP90 adopts an open conformation (V-shaped form). ATP induces conformational changes of HSP90 from open to closed form [30, 31].

In the present study, we have demonstrated the direct interaction of bHLH, HSP90, XAP2, and p23. We have also determined bHLH is the binding domain of HSP90-N domain as same as AhR-PAS. ATP did not affect the interaction of bHLH, HSP90, XAP2, and p23. Interestingly, 17-DMAG did not affect on the interaction between bHLH and HSP90. We have recently reported that HSP90 was dissociated from AhR-PAS in the presence of 17-DMAG [13]. The binding sites of bHLH and PAS to the HSP90 N-domain are slightly different each other. We speculate that the bHLH binding site of the HSP90 N-domain may be neighbor of the M-domain. On the contrary, the PAS binding site of the HSP90 N-domain may be end of the N-domain. ATP induces

dramatically conformational changes of HSP90 from open to closed form. The conformational change of HSP90N end is bigger than that of HSP90N neighbor M domain. The differences of 17-DMAG to bHLH and PAS are thought to be due to such reasons. We propose the models of the AhR-HSP90 chaperone complex (Fig. 13).
Based on the result, we inferred that HSP90 covers NLS when AhR is in the ligand-free state, and the conformational change of AhR complex lead to the exposure of NLS after AhR binds to ligand. For that reason, the AhR-bHLH domain interacts with HSP90. From the above, the AhR-bHLH domain is essential in the AhR activation mechanism similar to the PAS domain.

4.2 Analysis of AhR activation and function in human cells.

A novel AhR ligand DHNA is proposed to be non-toxic, we examined AhR activation by DHNA and the immunostimulating effect via AhR activation in human cell lines. As compared with 3MC, DHNA was not toxic for the cell viability and slightly increased cell population (data not shown), induction period of CYP1A1 was shorter than 3MC. Then we observed the translocation of AhR-HSP90 complex by immunofluorescence and proximity ligation assay (PLA), p23 did not translocate into the nucleus by DHNA, which indicates that DHNA as non-toxic ligand is recognized by different components of AhR-HSP90 complex, and from this result we hypothesize that AhR can subtly change its conformation for a diversity to accept several ligands. We propose the model of component differences of AhR-HSP90 chaperone complex in toxic and non-toxic ligands (Fig. 13). However, there remains two possibilities. First, DHNA are only recognized and binds to the complex which does not contain p23 then the complex translocates into nucleus. Second, DHNA binds to the known complex then p23 separates from the complex before the nuclear translocation. These are difficult to distinguish precisely so far. To solve this problem, we need further experiments such as time-lapse immunofluorescence observation and analysis of CYP1A1 expression under the knockdown of p23.

And in this study, we found that both 3MC and DHNA induced IL-12 and IFN-γ in the epithelial Caco-2 cells. This result indicates that when we uptake DHNA or *propionibacterium* itself, our intestinal immune system will be activated without toxicity of known AhR activity. This new insight will be needed further experiment using a co-culture model of Caco-2 cells and macrophage-like immune cells.

Acknowledgement

I would like to thank Prof. Hideaki Itoh of Department Life Science of Akita University for all his support, kindly accepted me to join into his laboratory, expertise and guidance throughout the study.

And I also thank to all members belonging to Prof. Itoh's laboratory for their assistance.

Finally, I'd like to give my all thanks to my family for encouraging me for a long time until graduate.

References

[1] Kewley R.J., Whitelaw M.L., Chapman-Smith A. (2004) The mammalian basic helix-loop-helix/PAS family of transcriptional regulators. *Int. J. Biochem. Cell Biol*. **36**, 189-204.

[2] Sorg O. (2014) AhR signaling and dioxin toxicity. *Toxicol. Lett.* **230**, 225-233.

[3] Mimura J., Fujii-Kuriyama Y. (2003) Functional role of AhR in the expression of toxic effects by TCDD. *Biochim. et Biophys. Acta* **1619**, 263-268.

[4] Nebert D.W., Gonzalez F.J. (1987) P450 genes: structure, evolution, and regulation. *Annu. Rev. Biochem.* **56**, 945-993.

[5] Kobayashi A, Sogawa K, Fujii-Kuriyama Y. (1996) Cooperative interaction between AhR·Arnt and Sp1 for the drug-inducible expression of CYP1A1 gene. *J. Biol. Chem.* **271**, 12310-12316.

[6] Beischlag T.V., Luis Morales J., Hollingshead B.D., and Perdew G.H. (2008) The aryl hydrocarbon receptor complex and the control of gene expression. *Crit. Rev. Eukaryot. Gene Expr.* **18**, 207-250

[7] Lees M.J., Whitelaw M.L. (1999) Multiple roles of ligand in transforming the dioxin receptor to an active basic helix-loop-helix/PAS transcription factor complex with the nuclear protein Arnt. *Mol. Cell. Biol.* **19**, 5811–5822.

[8] Taylor B.L., Zhulin I.B. (1999) PAS domains: internal sensors of oxygen, redox potential, and light. Microbiol. *Mol. Biol. Rev.* **63**, 479–506.

[9] Gu Y.Z., Hogenesch J.B., Bradfield C.A. (2000) The PAS superfamily: sensors of environmental and developmental signals. *Annu. Rev. Pharmacol. Toxicol.* **40**, 51961.

[10] McGuire J., Coumailleau P., Whitelaw M.L., Gustafsson J.A., Poellinger, L. (1995) The basic helix-loop-helix/PAS factor Sim is associated with hsp90. Implications for regulation by interaction with partner factors. *J. Biol Chem.* **270**, 31353-31357.

[11] Antonsson C., Arulampalam V., Whitelaw M.L., Pettersson S., Poellinger L. (1995) Constitutive function of the basic helix-loop-helix/PAS factor Arnt. Regulation of target promoters via the E box motif. *J. Biol Chem.* **270**, 13968-13972.

[12] Kazlauskas A., Poellinger L., and Pongratz I. (2000) The immunophilin-like protein XAP2 regulates ubiquitination and subcellular localization of the dioxin receptor. *J. Biol Chem.* **275**, 41317-41324.

[13] Tsuji N., Fukuda K., Nagata Y., Okada H., Haga A., Hatakeyama S., Yoshida S., Okamoto T., Hosaka M., Sekine K., Ohtaka K., Yamamoto S., Otaka M., Grave E., Itoh H. (2014) The activation mechanism of the aryl hydrocarbon receptor (AhR) by molecular chaperone HSP90. *FEBS Open Bio.* **4**, 796-803.

[14] Fukunaga B.N., Probst M.R., Reisz-Porszasz S., Hankinson O. (1995) Identification of functional domain of the aryl hydrocarbon receptor. *J Biol Chem.* **270**, 29270-29278.

[15] Whitley D., Goldberg S.P., Jordan W.D. (1999) Heat shock proteins: A review of the molecular chaperones. *J. Vasc. Surg.* **29**, 748-51.

[16] Lindquist S. (1986) The heat-shock response. *Annu. Rev. Biochem.* **55**, 1151-1191.

[17] Clare D.K., Saibil H.R. (2013) ATP-driven molecular chaperone machines. *Biopolymers* **99**, 846-859.

[18] Li J., Buchner J. (2013) Structure, function and regulation of the hsp90 machinery. *Biomed. J.* **36**, 106-117.

[19] Stejskalova L., Dvorak Z., Pavek P. (2011) Endogenous and exogenous ligands of aryl hydrocarbon receptor: current state of art. *Current Drug Metabolism* **12**, 198-212.

[20] Li X-m., Peng J., Gu W., Guo X-j. (2016) TCDD-induced activation of aryl hydrocarbon receptor inhibits Th17 polarization and regulates non-eosinophilic airway inflammation in asthma. *Plos One* **11(3)**.

[21] Takamura T., Harama D., Matsuoka S., Shimokawa N., Nakamura Y., Okumura K., Ogwa H., Kitamura M., Nakao A. (2010) Activation of the aryl hydrocarbon receptor pathway may ameliorate dextran sodium sulfate-induced colitis in mice. *Immun. and Cell. Biol*. **88**, 685-689.

[22] Isawa K., Hojo K., Yoda N., Kamiyama T., Makino S., Saito M., Sugano H., Mizoguchi C., Kurama S., Shibasaki M., Endo N., Sato Y. (2002) Isolation and identification of a new bifidogenic growth stimulator produced by *propionibacterium freudenreichii* ET-3. *Biosci. Biotechnol. Biochem.* **66 (3)**, 679-681.

[23] Fukumoto S., Toshimitsu T., Matsuoka S., Maruyama A., Oh-oka K., Takamura T., Nakamura Y., Ishimaru K., Fujii-Kuriyama Y., Ikegami S., Itou H., Nakao A. (2014) Identification of a probiotic bacteria-derived activator of the hydrocarbon receptor that inhibits colitis. *Immunol. Cell Biol.* **92**, 460-465.

[24] Lakhman S.S., Chen X., Gonzalez-Covarrubias V., Schuetz E.G., and Blanco J.G. (2007) Functional characterization of the promoter of human carbonyl reductase 1 (CBR1). Role of XRE elements in mediating the induction of CBR1 by ligands of the aryl hydrocarbon receptor. *Mol Pharmacol.* **72**, 734-743.

[25] Ali M.M., Roe S.M., Vaughan C.K., Meyer P., Panaretou B., Piper P.W., Prodromou C., Pearl L.H. (2006) Crystal structure of an Hsp90-nucleotide-p23/Sba1 closed chaperone complex. *Nature* **440**,1013-1017.

[26] Itoh H., Komatsuda A., Wakui H., Miura A.B., Tashima Y. (1999) Mammalian HSP60 is a major target for an immunosuppressant mizoribine. *J Biol Chem.* **274**, 35147-35151.

[27] Itoh H., Ogura M., Komatsuda A., Wakui H., Miura A.B., Tashima Y. (1999) A novel chaperone-activity-reducing mechanism of the 90-kDa molecular chaperone HSP90. *Biochem J.* **343**, 697-703.

[28] Ishida R., Takaoka Y., Yamamoto S., Miyazaki T., Otaka M., Watanabe S., Komatsuda A., Wakui H., Sawada K., Kubota H., Itoh, H. (2008) Cisplatin differently affects amino terminal and carboxyl terminal domains of HSP90. *FEBS Lett.* **582**, 3879-3883.

[29] Miyazaki T., Sagawa R., Honma T., Noguchi S., Harada T., Komatsuda A., Ohtani H., Wakui H., Sawada K., Otaka M., Watanabe S., Jikei M., Ogawa N., Hamada F., Itoh, H. (2004) 73-kDa molecular chaperone HSP73 is a direct target of antibiotic gentamicin. *J Biol Chem.* **279**, 17295-17300.

[30] Saibil H. (2013) Chaperone machines for protein folding, unfolding and disaggregation. *Nat Rev Mol Cell Biol.* **14**, 630-642.

[31] Röhl A., Rohrberg J., Buchner, J. (2013) The chaperone Hsp90: changing partners for demanding clients. *Trends Biochem Sci.* **38**, 253-262.